Marine and Petroleum Geology 156 (2023) 106448

Contents lists available at ScienceDirect

Marine and Petroleum Geology

journal homepage: www.elsevier.com/locate/marpetgeo

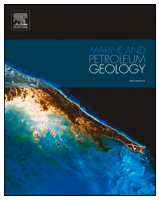

Maceral and calcareous nannofossil assemblages as proxies of late Rupelian (Oligocene) environmental changes in the Paratethys: An example from a section of the Menilite Formation in the northern Outer Carpathians

Patrycja Wójcik-Tabol [a], Marta Oszczypko-Clowes [a,*], Alfred Uchman [a], Weronika Pratkowiecka [a,b], Beata Dziubińska [a]

[a] Jagiellonian University, Faculty of Geography and Geology, Institute of Geological Sciences, Gronostajowa 3a, 30-387, Kraków, Poland
[b] Polish Geological Institute, National Research Institute, Jaworowa 19, 53-122, Wrocław, Poland

ARTICLE INFO

Keywords:
Organic matter
Nannofossils
Brackish waters
Black shale facies
Marls
Biostratigraphy
Lithostratigraphy

ABSTRACT

The Menilite Formation (Oligocene) of the Skole Nappe in the Polish Carpathians was deposited in the Paratethys. Deep-sea unbioturbated fine-grained carbonates of the Dynów Marl Member contain cold-water calcareous nannoplankton from Zone NP23 (Rupelian), including *Reticulofenestra ornata* and *Pontosphaera fibula*, which are typical of brackish waters in the Paratethys. It is likely that the water column was brackish in the upper part and fully marine and anoxic in the lower part. The Dynów Marl Member records the maximum isolation of the Paratethys from the oceanic circulation (the Upper Solenovian Event). The overlying green mudstones (probably the Krępak Member) are shallowly bioturbated. They contain fully marine, warm-water calcareous nannoplankton from Zone NP24. The environmental change (marine/brackish) is reflected in the quantity and type of organic matter. The abundance and preservation of organic matter are very high (TOC varies from 2.7 wt % to 26 wt %; HI values are >300 mg HC/g TOC) in brown, laminated shales, which were accumulated in saline anoxic conditions. The macerals in the shales are predominantly composed of the liptinite group, including lamalginite, telalginite, liptodetrinite, and bituminite. These macerals are primarily derived from planktonic and benthic algae as well as bacteria. The percentages of vitrinite and inertinite, originating from terrestrial sources, range up to 10% and 0.5%, respectively. The macerals are much less abundant in marls of the Dynów Marl Member because of dispersion in the carbonate groundmass during the calcareous nannoplankton blooms in brackish surface waters. The overall liptinite (mainly liptodetrinite and lamalginite) contribution is 77%–99.7%. Vitrinite and inertinite contents are in average 4.6% and 0.3%, respectively. Macerals are also infrequent in the overlying green mudstones, likely because of oxidation and consumption by organisms in warmer waters.

1. Introduction

The Paratethys sea stretched from Middle Europe to Middle Asia (e.g., Rögl, 1999; Popov et al., 2004), and became essentially isolated since the Early Oligocene (Báldi, 1980; Rusu, 1988; Rögl, 1999). The isolation, in combination with various local or wider factors (e.g., climatic/productivity changes), caused significant changes in salinity, water circulation, organic production, or oxygenation. Recognition of their complexity, duration, stratigraphy or paleogeographic context are still a matter of debate, e.g. oxygen minimum zone (e.g., Vető, 1987) versus the Black Sea model (e.g., Soták, 2010) in oxygenation of the basin. A better understanding of these issues is important because Oligocene organic-rich deposits in the Paratethys are among the important source rocks for hydrocarbons of this stratigraphic period (Wójcik-Tabol et al., 2022, and references therein). This also concerns the Oligocene of the Carpathians, whose basins/sub-basins were a part of the Paratethys at that time (Kováč et al., 2016, 2017a, and references therein). Here, the water circulation, oxygenation regime and bioproductivity have been studied, among others, by means of organic and inorganic geochemistry (e.g., Köster et al., 1998; Bechtel et al., 2012; Sachsenhofer et al., 2015; Kosakowski et al., 2018; Jirman et al., 2019; Rauball et al., 2019; Wójcik-Tabol et al., 2022), as well as paleontological, ichnological, sedimentological and microfacies analyses (e.g., Soták, 2010; Kotlarczyk and Uchman, 2012; Kováč et al., 2017b; Bojanowski et al., 2018, 2021).

* Corresponding author.
E-mail address: m.oszczypko-clowes@uj.edu.pl (M. Oszczypko-Clowes).

https://doi.org/10.1016/j.marpetgeo.2023.106448
Received 12 April 2023; Received in revised form 28 July 2023; Accepted 3 August 2023
Available online 6 August 2023

The organic-rich deposits of the Oligocene Paratethys are related to high productivity in the oxygen minimum zone, which commonly caused anoxia (e.g., Vető, 1987) or to the accumulation of organic matter in a stagnant basin (the Black Sea model, e.g., Soták, 2010). However, detailed ichnological and ichtiological investigations in the Skole Nappe in Poland (Kotlarczyk and Uchman, 2012) showed that both models can be applied for different time intervals in the same basin. The widespread and strongest anoxia in the Paratethys occurred in the middle of the NP23 Zone, and the Black Sea model was applied for its explanation, but with different water masses responsible for the stagnation. Strakhov (1971, 1976) or Deuser (1974) postulated incursions of heavy Mediterranean waters in the old Black Sea region, while Bośniacki (1911) and Soták (2010) proposed incursions of heavy cold boreal waters from the north, which underflowed lighter warm Mediterranean waters (Bośniacki, 1911) or were overflowed by lighter waters from lands located to the north (Soták (2010). The brackishness of surface waters in the Paratethys is a matter of debate (e.g., Kotlarczyk and Uchman, 2012; Filipek, 2020). It seems that since the early Rupelian cooling (e.g., Zachos et al., 2001; O'Brien et al., 2020), the incursions of boreal cold waters into the semi-isolated Paratethys and their elevation on submarine highs to the photic zone were a key factor in high organic productivity and the accumulation of organic-rich deposits; the Chattian climatic warming gradually stopped this process (Kotlarczyk and Uchman, 2012).

During the Late Rupelian, significant changes in salinity and organic production took place in the Paratethys (Kováč et al., 2016, 2017a, and references therein). In this paper, combined analyses of the petrology of organic matter (maceral assemblages) and the calcareous nannofossils are presented for interpretation of the environmental changes in the upper part of the Lower Oligocene (Upper Rupelian) fine-grained clastic and calcareous deep-sea deposits of the Menilite Formation from a selected section in the northern Carpathians in Poland (Tarnawka section in the Skole Nappe). Such a combination, especially with an application of macerals, has never been used for this purpose. The calcareous nannofossils were also used for the stratigraphic refining of the investigated deposits, which is essential for the correlation of the salinity changes in the Paratethys. The interpreted salinity changes are important to acquire a better understanding of the organic matter preservation of the Menilite Formation, which is well known for its hydrocarbon potential (e.g., Wójcik-Tabol et al., 2022). The organic petrography in the Oligocene of the Carpathians' successions has been mainly used as an indicator of organic matter origin and hydrocarbon potential (Kruge et al., 1996; Puglisi et al., 2006; Miclăus et al., 2009; Belkin et al., 2010; Waliczek and Więcław, 2012; Wójcik-Tabol, 2015, 2017; Wendorff et al., 2017; Kosakowski et al., 2018; Ziemianin, 2018, 2020; Zielińska et al., 2020; Waliczek et al., 2022).

2. Geological setting

The studied section is located in the Skole Nappe, which belongs to the flysch zone of the Eastern Carpathians, or, according to some divisions, of the Western Carpathians (the so-called Outer Carpathians). The Outer Carpathians are a fold-and-thrust belt (Fig. 1A and B) composed of a few stacked nappes completely uprooted from their substratum, which formed during the southward-directed subduction of the European plate under the Eastern Alpine–Western Carpathian–Northern Pannonian (ALCAPA) units (e.g., Oszczypko, 1999, 2006; Schmid et al., 2008; Kováč et al., 2016, 2017a; Golonka et al., 2019). The nappes consist of Upper Jurassic–Lower Miocene deposits that are mainly turbidities and other gravity flows, and less commonly hemipelagic or pelagic in origin (Książkiewicz, 1977; Żytko et al., 1989; Oszczypko, 2006).

The Skole Nappe occupies the outermost position of the Outer Carpathians in Poland. It consists of several elongated thrust-sheets and thrust folds (Fig. 1B and C), which contain Lower Cretaceous–Miocene deep-sea, mainly turbiditie. They accumulated in the Skole Basin, which was a trough bordered by the European Platform to the north and by the Subsilesian ridge and slope (now the Subsilesian Nappe) to the south (Golonka et al., 2019). The youngest deposits of the Skole Nappe belong to the Menilite–Krosno Series, which is composed of the Oligocene Menilite Formation, which contains, among others, black or dark brown non-calcareous shales, followed by the Oligocene–Miocene Krosno Formation dominated by yellow-weathering calcareous sandstones and mudstones (Kotlarczyk, 1988). This series, or its equivalents, are also known from other Carpathian nappes. The Menilite Formation of the Carpathians is an analogue of the Maikop Series in the Greater Caucasus, the Schoeneck Formation of the Alpine Foreland Basin, the Tard Clay of the Pannonian Basin and the Bulgarian Ruslar Formation which are examples of the Oligocene marine and estuarine successions in the Central and Eastern Paratethys (Schulz et al., 2004; Sachsenhofer et al., 2009).

The Menilite Formation (also called the Menilite Beds, fr. Couches à Menilite, or ger. Menilitenschichten in the literature) in the Skole Nappe is up to 400 m thick (Kotlarczyk and Uchman, 2012). It is dominated by brown or black, non-calcareous, organic-rich mudstones, which show variable fissility and are rich in fossil fishes (Kotlarczyk et al., 2006). Subordinately, this formation contains sandstones, conglomerates, dark grey siltstones, marlstones, horizons of coccolithic limestones, cherts, diatomites, and green mudstones (e.g., Kotlarczyk and Leśniak, 1990). The lithostratigraphy of the Menilite–Krosno Series in the Skole Nappe was presented by Kotlarczyk and Leśniak (1990) and Kotlarczyk, in Kotlarczyk et al. (2006). This lithostratigraphy scheme was a matter of controversy (Malata, 1996, 2006). A simpler lithostratigraphic scheme for the Oligocene of the Skole Nappe, with a smaller number of subdivisions, was presented by Jankowski et al. (2012), but those authors failed to discuss their scheme in the light of the more refined scheme proposed by Kotlarczyk et al. (2006). The latter, with its modified version by Kotlarczyk and Uchman (2012) is subjected to further corrections in this paper on the basis of the investigated section. A biostratigraphy of the Menilite-Krosno succession, based on nannofossils was proposed by Garecka (2008, 2012) who distinguished nannofossil zones from NP23 to NN4.

Material of the thicker sandstones was transported to the south from the European Platform foreland through channel zones to the Skole Basin by variable gravity flows (Kotlarczyk and Leśniak, 1990). At least a large part of the siltstones and mudstones were also deposited by gravity flows, but some thin sandstone or siltstone intercalations were deposited by bottom traction currents (Unrug, 1980). Some interpretations favoring the shallow-marine environment of the Menilite Formation within the range of storm currents or even shallower zones (e.g., Nalivkin, 1963, 1967; Jarmołowicz-Szulc and Jankowski, 2011; Jankowski, 2015; Jankowski and Wysocka, 2019; Filipek, 2020) are not convincing (for the discussion, see Salata and Uchman, 2019).

The investigated section (Fig. 1C and 2) is unique because the base and top of the Dynów Marl Member and the underlying and overlying deposits are exposed here. In other exposers of the Menilite Formation in the Skole Nappe, at least one of the elements is missing. It is located in an abandoned quarry at Tarnawka (N49°56.891', E22°16.840'), where the lower part of the Menilite Formation is exposed. Here, the beds are dipping steeply to the south-west. In the lowermost part of section (2.8 m), thin layers of grey marls are intercalated with brown or black mudstones and with a few beds of very fine-to medium-grained sandstones. They belong to the Strwiąż Globigerina Marl Member of the Hieroglyphic Formation; the Eocene-Oligocene boundary is somewhere within this unit (Rajchel, 1990). Up the section, they transit to a 4.2 m-thick package of brown or black mudstones and thin-bedded very fine, occasionally medium or very coarse-grained sandstones belonging to the Jamna Dolna Member (Fig. 2). Above, a ca. 15–16 m-thick package of thick- and medium-bedded sandstones is intercalated by thin-to-thick intercalations of siltstones/mudstones. This package belongs to the Boryslav Member (Fig. 2). The sandstones are light grey and beige, slightly greenish in color, massive and brittle. They are

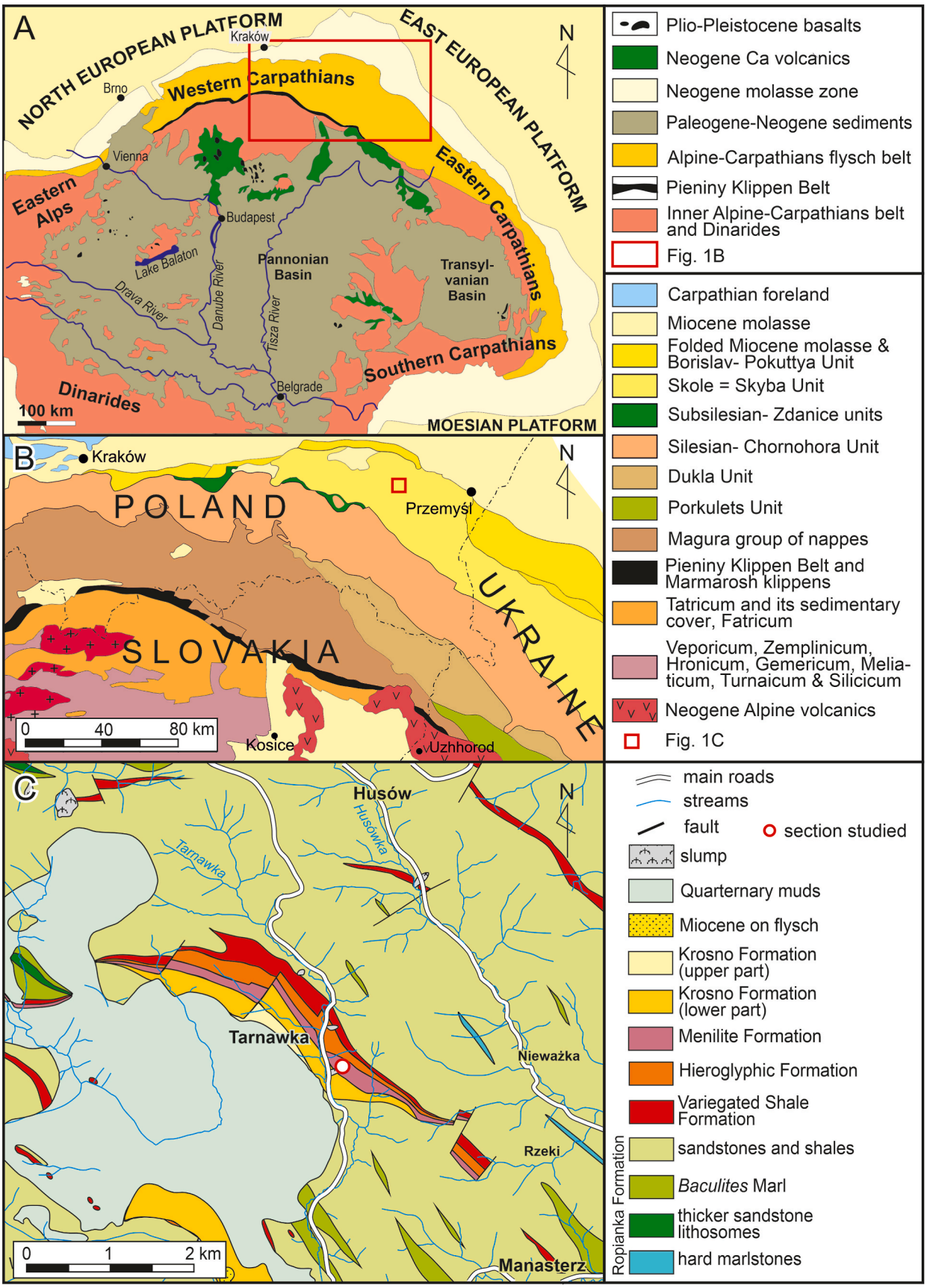

Fig. 1. Location maps: (A) tectonic sketch-map of the Alpine–Carpathian–Pannonian area (after Schmid et al., 2008); (B) tectonic sketch-map of the Western Carpathians and adjacent Ukrainian Carpathians (based on Oszczypko and Oszczypko-Clowes, 2009); (C) geological map of Skole Nappe in the study area in Poland (based on Wdowiarz, 1949).

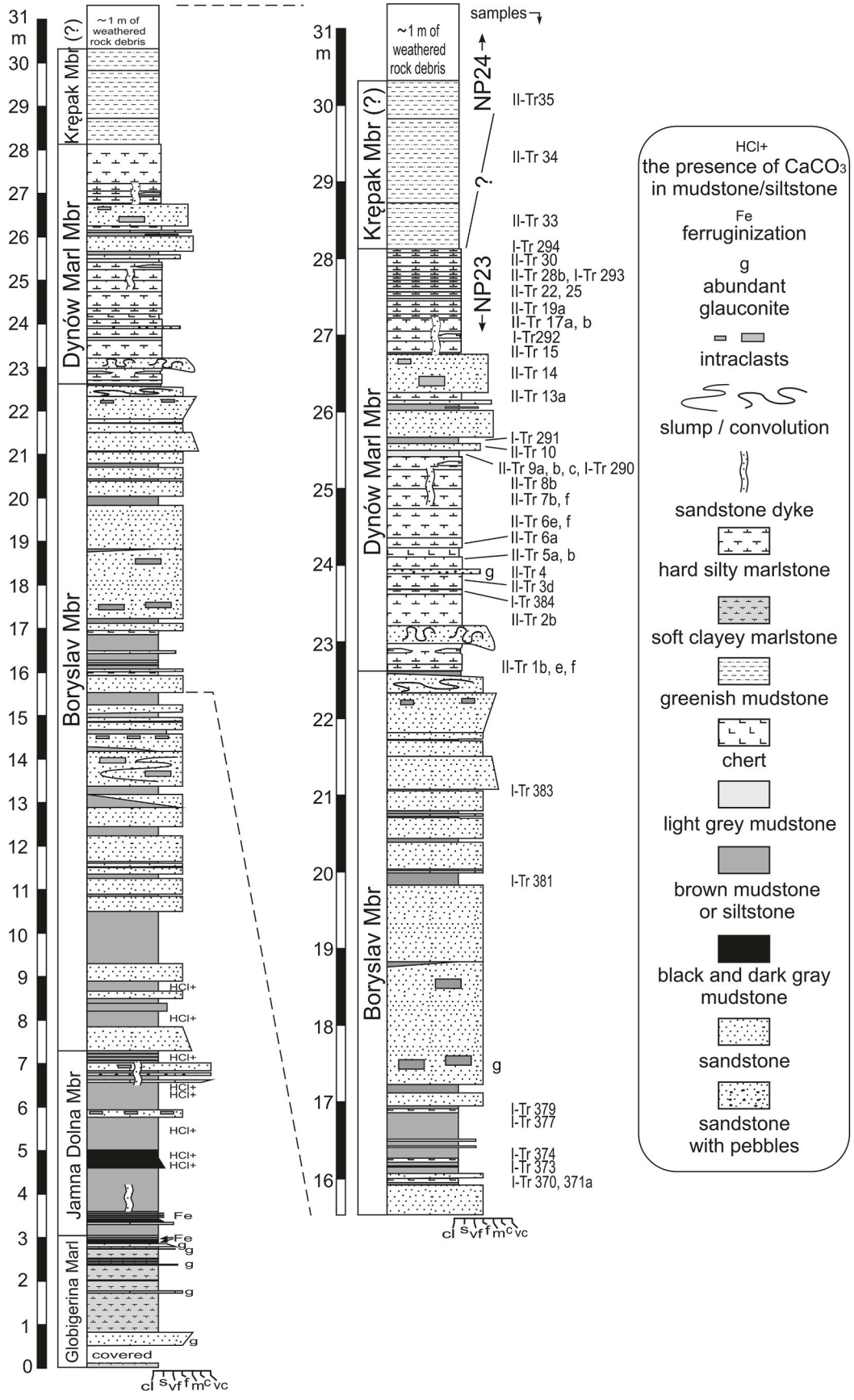

Fig. 2. Lithostratigraphic log of the Menilite Formation in the Tarnawka section, with the samples' locality.

fine-to-coarse grained, normally or inversely graded, non-calcareous and siliceous, locally with glauconite. Grains of quartz and feldspar are macroscopically recognisable (quartz arenites; cf. Salata and Uchman, 2012). Several sandstone beds hold intraclasts of brown shales, cherts, and coals. The siltstone/mudstone intercalations of the sandstone beds are brown, black or grey non-calcareous and siliceous, non-bioturbated, locally with subtle parallel lamination. Due to their leaf-like, thin-plate, and plate fissility, they are called shales. They contain carbonised plant debris and commonly fine fish remains (scales and bones). Their dark brown colors and specific (bituminous) smell indicate a high content of organic matter. The yellow coating on the fissility surfaces suggests that the shales contain iron sulphides that have been transformed into jarosite as a result of weathering.

A few beds in the middle and upper parts of the package (1.8 m) are deformed by a submarine slump. This unit in the studied section was erroneously ascribed to the Kliva Member (Malata, 2006), but the Kliva Member (quartz arenites) is exposed about 1.2 km away and occupies a distinctly higher stratigraphic position. According to the stratigraphic scheme, the Boryslav Member should be followed by thin-bedded chert and shales of the Kotów Chert Member (cf. Kotlarczyk and Leśniak, 1990). However, in the Tarnawka section, this unit is only manifested by a few diffused thin layers of cherts in mudstone/siltstone intercalations between sandstone beds of the Boryslav Member.

Directly above the Boryslav Member is a package (5.5 m thick) of bedded siliceous marls, marlstones, and marly limestones (for simplicity, hereinafter referred to as marls), with a few beds of non-glauconitic and one bed of glauconitic sandstones, and shale and chert intercalations. This package belongs to the Dynów Marl Member (Fig. 2). Some beds of marls show shale fissility, especially in the upper 1 m-thick interval. The rocks are parallel laminated or non-laminated. Lamination occurs in the bottom or top parts of the beds. The laminae are grey, beige, white, or rusty in color, about 1 mm thick, and are often discontinuous with fuzzy boundaries. Grey marls are more siliceous and harder than beige marls and show indistinct wavy layering.

The exposed section ends with greenish, grey-green (referred to as green for simplicity), soft, calcareous mudstones, which are at least 2.2 m thick. They show tabular parting. Silt-sized quartz grains, fine flakes of muscovite, and black organic particles are dispersed in the clay matrix. The plasticity and stickiness of the mudstones suggest a high content of smectite. Their top is covered. The green mudstones do not fit into any lithostratigraphic unit in this stratigraphic position according to the lithostratigraphic scheme in Kotlarczyk et al. (2006). Above the Dynów Marl Member should be roughly at least 20–30 m of deposits belonging to the Rudawka Tractionite Member and the Borek Nowy Member, which contain mostly black, grey, and brown shales, with thin-bedded sandstones, cherts or diatomites. However, Kotlarczyk and Leśniak (1990) mentioned that the Rudawka Tractionite Member in the nearby Widaczów (6–7 km apart) is only 5 m thick. It is not discounted that this member and the Borek Nowy Member may be missing in the Tarnawka section due to erosion or non-deposition. The section is located in the Łańcut Channel Zone, which supplied sedimentary material from the north and north-west (Kotlarczyk and Leśniak, 1990), where such phenomena can be expected. The contact between is the Dynów Marl Member and the green mudstones is visible only at a distance of 1–2 m, and the possible record of erosion or depositional bypass does not need to be visible. Lithologically, the green mudstones are most similar to the Krępak Member (middle-upper part of Zone NP23 in Kotlarczyk et al., 2006), which is characterised by green clayey-siliceous mudstone shales with or without Kliva Member-like sandstones (Kotlarczyk and Leśniak, 1990).

3. Material and methods

3.1. Studied material

The presented investigations are focused on the environmental changes in late Rupelian. Therefore they are based on samples starting from mudstone intercalations in the upper part of the Boryslav Member and the Dynów Marl Member, up to the top of the exposed green mudstones (possibly the Krępak Member).

45 samples were collected for this investigation. The samples represent all lithotypes occurring in the section, that is, mudstone (14 samples including 9 from the Boryslav Member, 2 from the Dynów Marl Member and 3 from the Krępak Member), marl (28 samples), sandstone (3 samples from the Dynów Marl Member), and chert (laminae of chert in marl or mudstone). The location of the sampled section is given in Fig. 1, while a detailed lithostratigraphic column with the positions of the samples is shown in Fig. 2. Apart from Rock-Eval pyrolysis, the rest of the research was carried out at the Jagiellonian University.

3.2. Mineralogy and petrography

Petrological studies including description of mineral composition and rock texture were conducted in 21 thin sections (I-Tr 370, I-Tr 371a, I-Tr 374, I-Tr 377, I-Tr 379, I-Tr 383, II-Tr 1e, I-Tr 384, II-Tr 4, II-Tr 5b, II-Tr 6f, II-Tr 7b, II-Tr 9b, I-Tr 290, II-Tr 10, II-Tr 14, II-Tr 17a, II-Tr 25, I-Tr 294, II-Tr 33, II-Tr 34) of each lithotype using a Nikon-Eclipse Ni microscope. Macro- and micro-images of representative samples are shown in Fig. 3.

The total content of carbonates was determined in 12 samples of marl (II-Tr 1f, 5a, 6a, 6e, 9a, 15, I-Tr 292, II-Tr 19a, 25, I-Tr 293, II-Tr 28b, 30) by means of the Scheibler volumetric method (Lityński et al., 1976) using the calcimeter by Eijkelkamp that is suitable for the simultaneous determination of the carbonate content in 5 samples. The carbonates are converted to CO_2 by adding 4 M HCl (7 ml). As a result of the pressure of the released CO_2, the water in the burette rises. The ambient pressure and temperature were recorded for each sample to calculate the pT factor, which corrects the CO_2 volume. The carbonate content is expressed as calcium equivalent carbonate content.

3.3. Calcareous nannofossils

Twenty samples were prepared for nannofossil investigation (II-Tr 1b, II-Tr 2b, II-Tr 3d, II-Tr 5a, II-Tr 6a, II-Tr 7f, II-Tr 8b, I-Tr 291, II-Tr 13a, II-Tr 17 b, II-Tr 19a, II-Tr 22, II-Tr 25, II-Tr 28, I-Tr 384, I-Tr 293, I-Tr 294, II-Tr 33–35), using the standard smear slide technique (Bown, 1998) for a light microscope. All samples were analysed with a Nikon-Eclipse E 600 POL, at a 1000x magnification using both parallel and crossed nicols. The most typical species were photographed and are presented in alphabetic order in Fig. 4 (A–Y). The determined species are presented in Table 1. Qualitative analyses allowed the age determination. The applied taxonomic frameworks were based upon Perch-Nielsen (1985, and references therein) and Bown (1998, and references therein). The biostratigraphy was based on the standard zonation of Martini (1971). However, the index species for the Oligocene zones were absent or very rare at high latitudes. In such cases, secondary index species had to be applied (Nagymarosy and Voronina, 1992; Śliwińska et al., 2012). To be able to describe state of nannofossil preservation, the criteria proposed by Roth and Thierstein (1972) were used namely: VP – very poor, etching and mechanical damage is very intensive, specimens mostly in fragments; P – poor, severe dissolution, fragmentation and/or overgrowth; the specific identification of specimens is difficult; M – moderate, etching or mechanical damage is apparent but majority of specimens are easily identifiable; G – good, little dissolution and/or overgrowth; diagnostic characteristics are preserved, the specimens could be identified to species level without any “trouble”. Estimates of the nannofossil abundance for individual samples (Table 1) was established using the following criteria: VH – very high (>20 specimens per 1 field of view), H – (10–20 specimens per 1 field of view), M – moderate (5–10 specimens per 1 field of view), L – low (1–5 specimens per 1 field of view), VL – very low (<5 specimens per 5 fields of view).

3.4. Rock-Eval pyrolysis and macerals

The total organic carbon contents (TOC) and hydrogen index (HI) in the samples of brown shales (I-Tr 370, 373, 380, 381, 383, 291, Tr-II 9C) were acquired using Rock-Eval 6 pyrolysis (Behar et al., 2001) in the Polish Geological Institute - National Research Institute. The HI is calculated using the formula HI = 100·S_2/TOC (mg/g TOC), where S_2 is the amount of bound hydrocarbons and non-hydrocarbon compounds that are released by pyrolysis. The contents of carbonates and TOC, and the distribution of macerals are given in Fig. 5.

Maceral examinations were carried out in thin sections made from 21 rock samples ((I-Tr 370, I-Tr 371a, I-Tr 374, I-Tr 377, I-Tr 379, I-Tr 383, II-Tr 1e, I-Tr 384, II-Tr 4, II-Tr 5b, II-Tr 6f, II-Tr 7b, II-Tr 9b, I-Tr 290, II-Tr 10, II-Tr 14, II-Tr 17a, II-Tr 25, I-Tr 294, II-Tr 33, II-Tr 34) of each

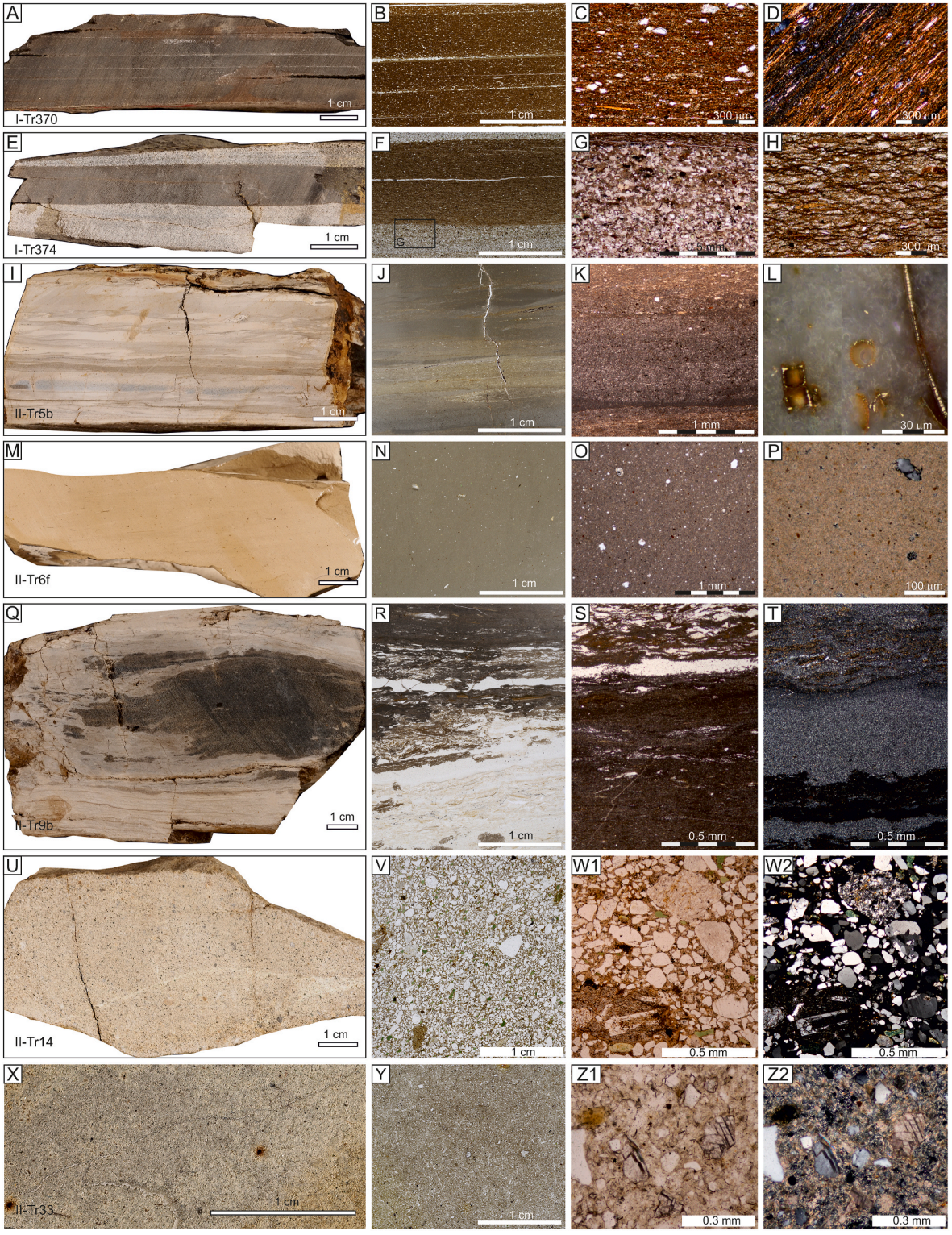

(caption on next page)

Fig. 3. Macro- and micro-images of samples from the Tarnawka section: (A–D) parallel laminated brown shale, sample I-Tr370; (B) silty grains dispersed in clayey-siliceous matrix, a planar parallel distribution of elongated forms and laminas of silt; (C) silty grains dispersed in clayey-siliceous matrix, a planar parallel distribution of elongated mineral and organic matter, PN; (D) silty grains of quartz, feldspar and mica dispersed in clayey-siliceous matrix, CN; (E–H) brown mudstone, sample I-Tr374; (E) silty layers poor in organic matter interbedded with brown shale; (F) brown mudstone intercalation between silty layers with G indicating the field of the G image; (G) thin-section image of silt, angular grains, rounded glauconite, fossils and organic detritus, PN; (H) thin-section photo of mudstone enriched in filamentous organic matter, PN; (I–L) laminated beige marlstone, sample II-Tr5b; (J) clastic and biogenic material in carbonate-clayey background, lamination related to the occurrence of silica, and the addition of clastic or opaque minerals, with K indicating the field of the K image; (K) thin-section photo of siliceous layer enriched in opaque minerals, PN; (L) pyritised microfossils, partly oxidised, with reflected light; (M–P) beige marlstone, sample II-Tr6f; (N) clastic and biogenic material loosely distributed in carbonate-clayey background; (O) foraminifera test and angular grains, PN; (P) quartz grains corroded by lime micrite, CN; (Q–T) grey siliceous marlstones; (R) zones of very fine-crystalline silica (Si) and carbonate-clay (Cc) matrix; (S) thin-section photo of siliceous and calcareous zones, PN; (T) thin-section photo of siliceous zone intercalated with carbonate (Cc) layers and carbonate minerals (C) admixture; (U–W2) sandstone sample II-Tr14; (U, V) poorly sorted greywacke comprised of quartz, glauconite and lithoclasts; (W1, W2) poorly rounded mono- and poly-crystalline quartz, clasts of igneous and metamorphic rocks, glauconite, and clayey-siliceous matrix, PN and CN, respectively; (X–Z2) green mudstones, sample II-Tr 33; (Y) silt grains chaotically dispersed in carbonate-clay matrix; (Z1, Z2) edgy-shape grains of quartz, feldspar, mica and carbonate dispersed in clayey-carbonate matrix, PN and CN, respectively. CN: crossed nicols; PN: parallel nicols.

lithotype. The most typical macerals are presented in Fig. 6. Fluorescent light (blue) was applied using the Nikon-Eclipse Ni microscope, equipped with a Prior Lumen 200 light source, an excitation filter (EX 450–490 nm), a dichroic mirror (DM 505 nm) and a barrier filter (BA 520 nm). The dispersed organic matter was classified in accordance with the International Committee for Coal and Organic Petrology (ICCP) System 1994; ICCP, 1998, 2001; Pickel et al., 2017). The point count method for maceral examination was conducted according to the Fleet method using a semi-automated point-counting stage. A minimum of 300 readings for chert and sandstone and 500 readings for mudstone and marl were recorded for the maceral analyses. Maceral frequencies were calculated as volume percentages.

4. Results

4.1. Mineral composition and petrography

In the thin sections, the brown shales (intercalations in the Boryslav and the Dynów Marl members) show planar parallel laminae emphasized by elongated organic matter (Fig. 3A–H). Clayey-siliceous matrix is the dominant groundmass of mudstones (Fig. 3C and D). The silt grains are loosely scattered in the matrix and concentrate in silty laminae and layers (Fig. 3E and F). The grains are represented by mineral detritus (quartz, mica, glauconite) and carbonised organic remains. The fossils (e.g., foraminifers and radiolaria, sponge spicules) are numerous in layers enriched with silty material (Fig. 3G). Organic matter is accompanied by pyrite which is shaped as tiny framboids (diameter of 3–5 μm).

The marls (Fig. 3I–P) consist mainly of a carbonate-clayey background and dispersed clastic and biogenic material, including pyritised fossils (Fig. 3L).

Some of marls are siliceous (Fig. 3Q) containing very fine-crystalline silica and carbonate-clay matrix (Fig. 3R–T).

The marls from the middle part of the Dynów Marl Member show the highest content of carbonates (Fig. 5). The decrease in carbonate contents in the siliceous marls and marly shales is caused by an increase in the content of silica or terrigenous detritus, respectively.

The sandstone intercalations within the Dynów Marl Member are developed as massive siliceous or siliceous-clayey, locally glauconitic sandstones that represent well-sorted feldspar lithoarenite or poorly sorted greywacke (Fig. 3U–W2).

The green mudstones from the upper part of the section (possibly the Krępak Member) (Fig. 3X, Y) are composed of a carbonate-clay matrix, in which the silt grains are chaotically dispersed. The grains are usually sharp-edged and poorly sorted (Fig. 3Z1, 3Z2).

4.2. Calcareous nannofossils

Almost all the samples from the Dynów Marl Member (II-Tr 1b, 2b, 3d, 5a, 6a, 7f, 8b, I-Tr 291, II-Tr 13a, 17b, 19a, 22, 25, 28; I-Tr 384, 293, 294) contain nearly monospecific nannofossil assemblage. The most abundant is *Reticulofenestra ornata* (Fig. 4V–X), whereas *Pontosphaera fibula* and *R. lockeri* are very rare. The preservation of calcareous nannofossils is poor to moderate, with signs of severe dissolution (Table 1). Such a state of preservation makes the specific identification of specimens difficult.

The nannofossil assemblage from Krępak Member, samples II-Tr 33–35 (green mudstone), is characterised by the presence of rich and diversified assemblages. The preservation of calcareous nannofossils is moderate (M) or predominantly moderate to good (G) in all the investigated samples. The nannofossils show minor etching and minor-to-moderate overgrowth. Good and moderate preservation of nannofossils indicates that little carbonate dissolution has occurred in these sediments. The nannofossil abundance in individual samples varies from moderate (M) to low (L). The assemblage is characterised by the presence of *Coccolithus pelagicus* (Fig. 4A and B), *Cyclicargolithus abisectus* greater than 12 μm (Fig. 4C–E), *Cyclicargolithus floridanus* (Fig. 4F), *Reticulofenestra bisecta* (Fig. 4G and H), *Helicosphaera carteri* (Fig. 4I–N), *H. compacta* (Fig. 4O, P), *H. ethologa*, *H. intermedia* (Fig. 4Q), *Ponthosphaera latoculata* (Fig. 4R), *P. multipora* (Fig. 4S), *R. dictyoda* (Fig. 4T), *R. lockeri* (Fig. 4U), *Sphenolithus moriformis* and *Zygrhablithus bijugatus* (Fig. 4Y).

4.3. The organic matter

The Rock-Eval parameters obtained from brown shales are presented in Table 2. Other lithotypes were not considered for the TOC measurement due to their color, which is indicative of a low organic matter content. TOC varies from 7.1 wt % to 26 wt % in shales of the Boryslav Member and from 2.7 to 6.7 wt% in shales of the Dynów Marl Member. Rock Eval analyses revealed hydrogen index (HI) values between 326 and 680 mg HC/g TOC (Table 2, Fig. 5). The Tmax values range from 410 to 430 °C. HI values above 500 mg HC/g TOC and Tmax below 420 °C are typical for the Boryslav Member, while brown shales interbedding the Dynów Marl Member show lower HI values and higher Tmax values (Table 2).

Maceral composition for the brown shales is characterised by a high content of liptinite group. The overall liptinite content is 89.3%–99.8% (Fig. 5). This group is represented by lamalginite, telalginite, liptodetrinite and bituminite. The lamalginite shows straight or bent and wrapped laminae with an average size of 8 × 140 μm (Fig. 6A). Telalginite (average dimensions: 28 × 213 μm) with a well-preserved internal structure (Fig. 6B and C) and singular liptodetrinite (average dimensions: 7 × 18 μm; Fig. 6A–C) were also recognised there. Bituminite is an amorphous organic matter admixed with mineral matrix. It is concentrated in elongated lenses, laminae or irregular bands. Bituminite is accompanied by alginite (Fig. 6A–C). Percentages of vitrinite and inertinite range up to 10% and 0.5%, respectively. Vitrinite and inertinite occur as angular or elongated debris, called vitrodetrinite and inertodetrinite (Fig. 6D). Occasionally, in a silt layer, cellular

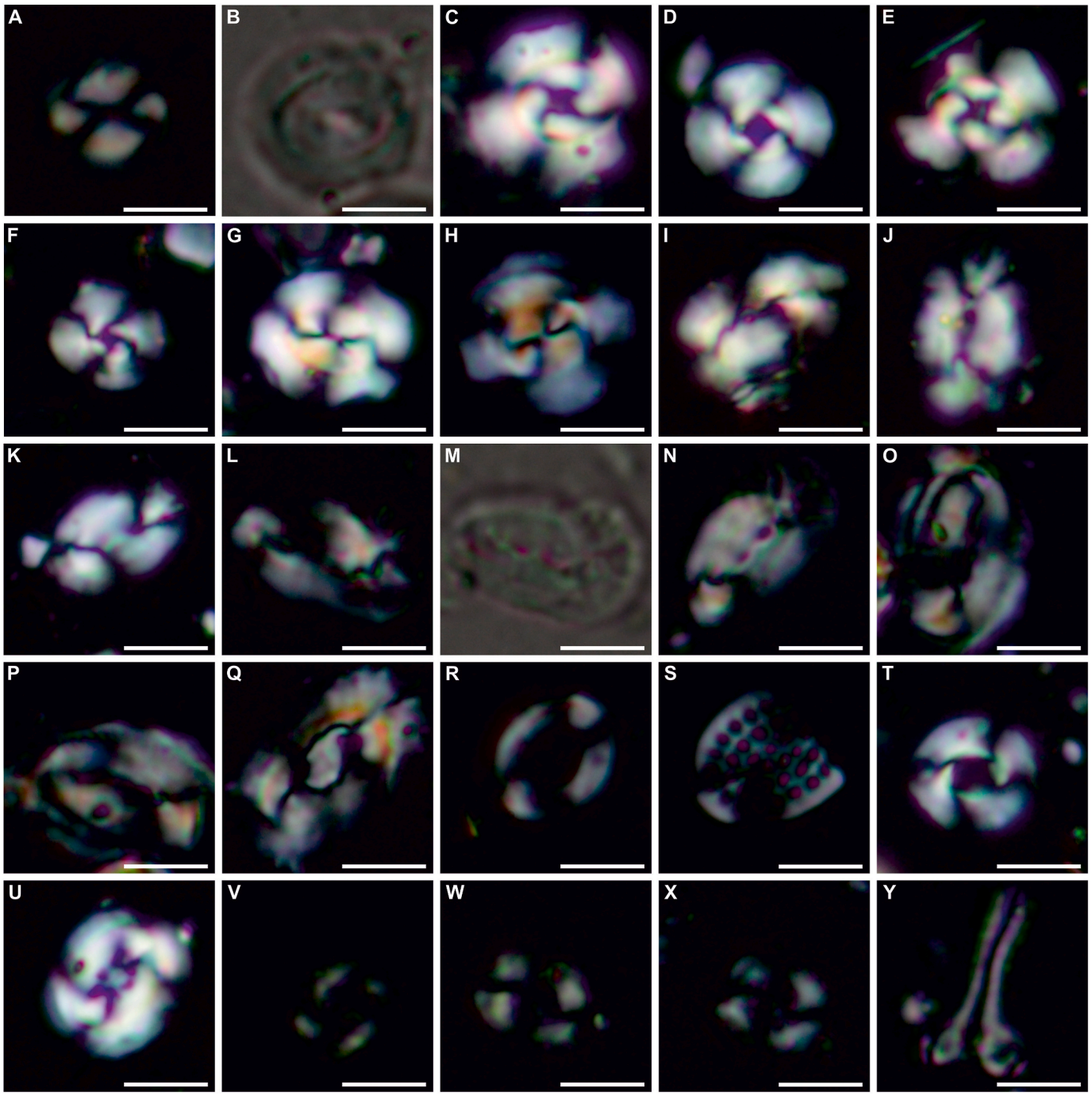

Fig. 4. Light microscope images of typical nannofossil species
(A) *Coccolithus pelagicus* sample II-Tr33, CN; (B) *Coccolithus pelagicus* sample II-Tr33, PN, (C) *Cyclicargolithus abisectus*, sample II-Tr33, CN; (D) *Cyclicargolithus abisectus*, sample II-Tr34, CN; (E) *Cyclicargolithus abisectus*, sample II-Tr35, CN; (F) *Cyclicargolithus floridanus*, sample II-Tr33, CN; (G) *Reticulofenestra bisecta*, sample II-Tr33, CN; (H) *Reticulofenestra bisecta*, sample II-Tr35, CN; (I) *Helicosphaera carteri*, sample II-Tr33, CN; (J) *Helicosphaera carteri*, sample II-Tr33, CN; (K) *Helicosphaera carteri*, sample II-Tr34, CN; (L) *Helicosphaera carteri*, sample II-Tr34, CN; (M) *Helicosphaera carteri*, sample II-Tr34, PN; (N) *Helicosphaera carteri*, sample II-Tr34, CN; (O) *Helicosphaera compacta*, sample II-Tr33, CN; (P) *Helicosphaera compacta*, sample II-Tr33, CN; (Q) *Helicosphaera intermedia*, sample II-Tr33, CN; (R) *Pontosphaera latoculata,* sample II-Tr33, CN; (S) *Pontosphaera multipora*, sample II-Tr33, CN; (T) *Reticulofenestra dictyoda*, sample II-Tr 2b, CN (U) *Reticulofenestra lockeri*, sample II-Tr33, CN; (V) *Reticulofenestra ornata*, sample II-Tr 1b, CN; (W) *Reticulofenestra ornata*, sample II-Tr 2b, CN; (X) *Reticulofenestra ornata*, sample II-Tr 8b, CN. (Y) *Zygrhablithus bijugatus*, sample II-Tr35, CN. Scale: 5 μm; CN: crossed nicols; PN: parallel nicols.

semifusinite and funginite are present (Fig. 6E and F). The brown shales intercalating the Dynów Marl Member contain a higher quantity of vitrinite and liptodetrinite compared to the shales of the Boryslav Member.

The organic matter in the cherts' intercalation in the brown shales (upper part of the Boryslav Member) is mainly represented by lamalginite filaments (average dimensions: 19 × 488 μm), telalginite (average dimensions: 32 × 208 μm) and liptodetrinite (average dimensions: 11 × 17 μm). The laminar distribution is characterised by the presence of a layer enriched in lamalginite passing into the zone with liptodetrinite (Fig. 6G). Vitrinite and inertinite occur very rarely.

The marl samples of the Dynów Marl Member contain mainly

Table 1
The distribution of calcareous nannoplankton in the Tarnawka section. X – autochthonous species, R – reworked.

	OLIGOCENE																			
tectonic unit/ lithostratigraphy	SKOLE NAPPE																			
	DYNÓW MARL MEMBER																	KRĘPAK MEMBER		
nannofossils zones Martini (1971)	NP23	NP23	NP23	NP23	NP23	NP23	NP23	NP23	NP23	NP23	NP23	NP23	NP23	NP23	NP23	NP23	NP23	NP24	NP24	NP24
sample number	II-Tr 1b	II-Tr 2b	II-Tr 3d	II-Tr 5a	II-Tr 6a	II-Tr 7f	II-Tr 8b	I-Tr 291	II-Tr 13a	II-Tr 17b	II-Tr 19a	II-Tr 22	II-Tr 25	II-Tr 28	I-Tr 384	I-Tr 293	I-Tr 294	II-Tr 33	II-Tr 34	II-Tr 35
sample abundance	M	L	L	L	M	M	L	M	L	L	L	L	L	M	M	M	M	L	M	M
nannofossil preservation	M	P	M	M	M	M	P	M	P	P	P	P	P	M	M	P	P	M	G	G
Coccolithus pelagicus																		X	X	X
Cyclicargolithus abisectus																		X	X	X
Cyclicargolithus floridanus																		X	X	X
Ericsonia fenestrata																		R	R	R
Ericsonia formosa																		R	R	R
Helicosphaera carteri																		X	X	X
Helicosphaera compacta																		X	X	X
Helicosphaera euphratis																		X	X	X
Helicosphaera ethologa																		X	X	X
Helicosphaera intermedia																		X	X	X
Lanternithus minutus																		X	X	X
Neococcolithes dubius																		R	R	R
Pontosphaera fibula	X	X		X				X				X		X	X	X	X	X	X	X
Pontosphaera latoculata																		X	X	X
Pontosphaera multipora																		X	X	X
Pontosphaera plana																		X	X	X
Pontosphaera pulchra																		X	X	X
Reticulofenestra bisecta	X	X	X	X	X	X	X	X	X	X	X	X	X	X	X	X	X	X	X	X
Reticulofenestra dictyoda																		X	X	X
Reticulofenestra lockerii	X	X	X	X		X			X		X	X	X	X			X	X	X	X
Reticulofenestra minuta																		X	X	X
Reticulofenestra ornata	X	X	X	X	X	X	X	X	X	X	X	X	X	X	X	X	X	X	X	X
Sphenolithus dissimilis																		X	X	X
Sphenolithus moriformis																		X	X	X
Sphenolithus pseudoradians																		R	R	R
Sphenolithus radians																		R	R	R
Zygrhablithus bijugatus																		X	X	X

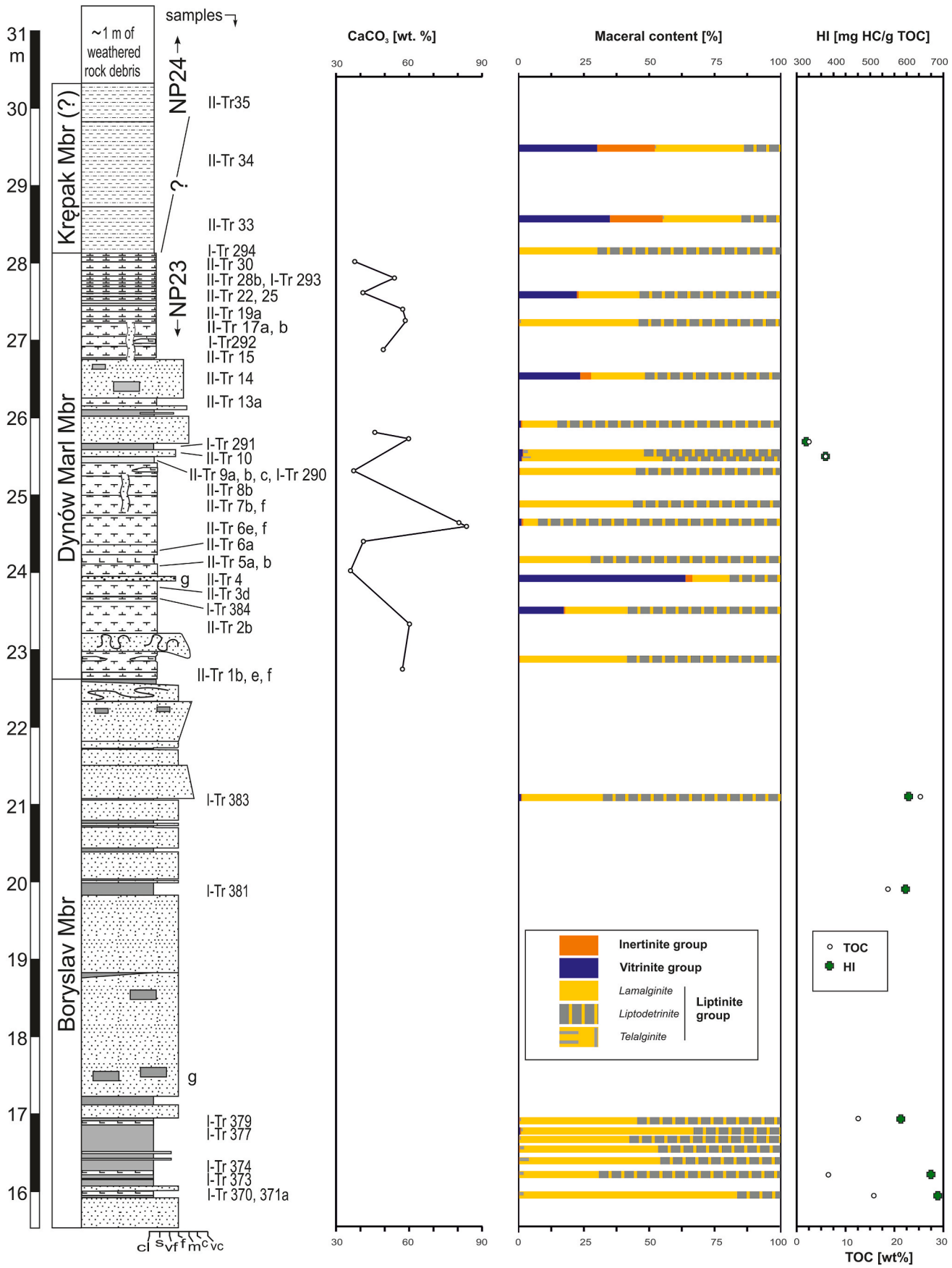

Fig. 5. Carbonate content tested by calcimetry; Rock-Eval characteristics and distribution of macerals in the Tarnawka section.

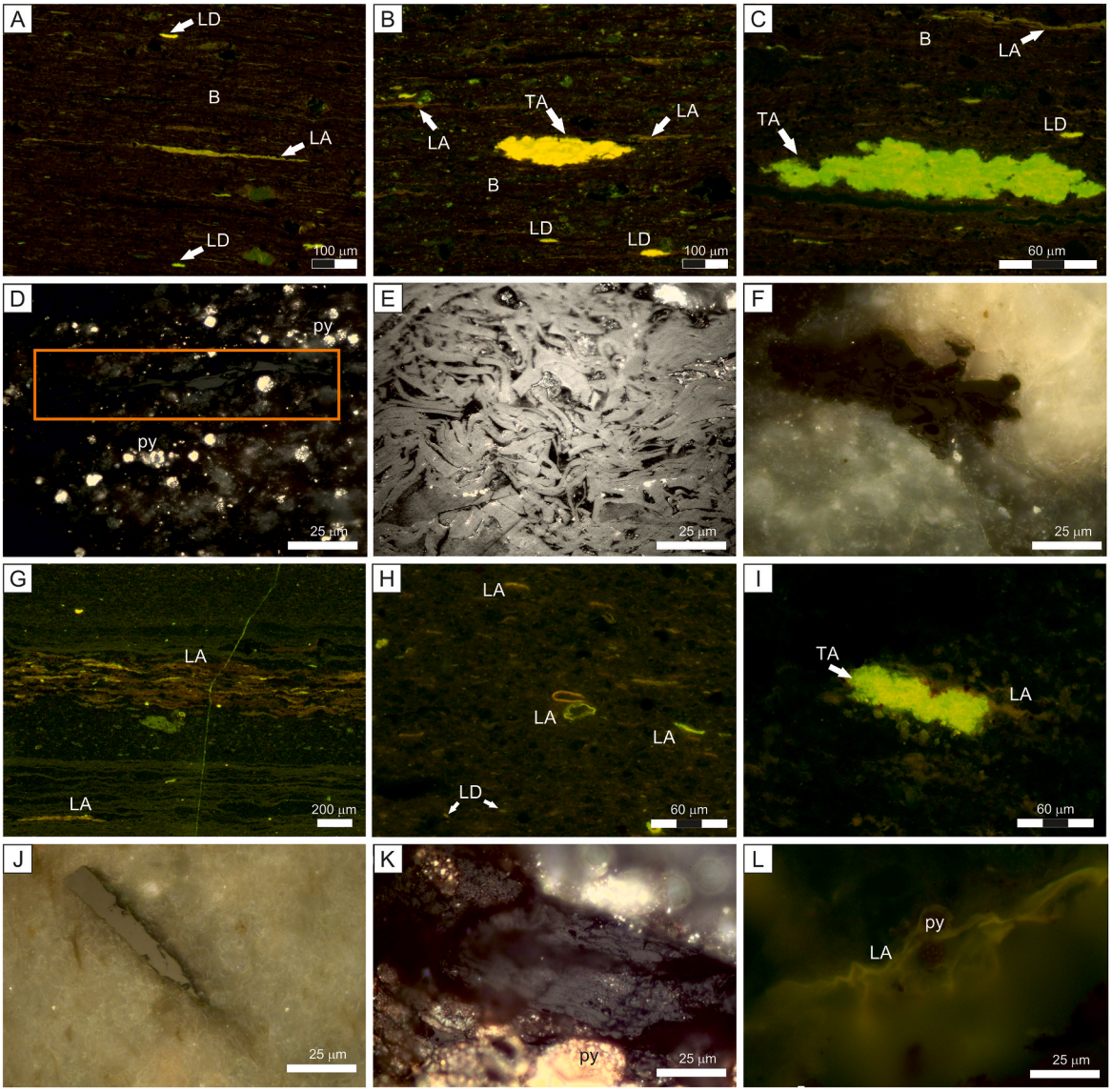

Fig. 6. Macerals from the Menilite Formation in the Tarnawka section: (A) lamalginite, bituminite and liptodetrinite, sample I-Tr381; (B) telalginite, lamalginite and bituminite, sample I-Tr371a; (C) telalginite, lamalginite, bituminite and liptodetrinite, sample I-Tr373; (D) elongated vitrodetrinite in rectangle, sample I-Tr370; (E) semifusinite, mudstone sample I-Tr374; (F) funginite, mudstone sample I-Tr377; (G) lamination, planar distribution of lamalginite, chert sample I-Tr377rog; (H) lamalginite, marl sample I-Tr294; (I) telalginite, marl sample II-Tr17a; (J) inertodetrinite, marl sample I-Tr294; (K) vitrinite and pyritisation, green shale sample II-Tr33; (L) lamalginite, green mudstone sample II-Tr33. D–F, J, K: reflected light; A–C, G–I, L: fluorescence illumination. Abbreviations: LA - lamalginite, TA – telalginite, B – bituminite, LD – liptodetrinite, py – pyrite.

Table 2
Pyrolysis Rock-Eval parameters.

sample	S_1	S_2	Tmax	HI	OI	TOC
	[mg HC/g rock]	[mg HC/g rock]	[°C]	[mg HC/g TOC]	[mg CO_2/g TOC]	[wt%]
I-Tr 370	3.36	105.29	418	680	25	15.5
I Tr 373	1.19	46.93	417	664	19	7.1
I-Tr 379	2.02	72.35	411	575	25	12.6
I-Tr 381	2.5	111.21	411	590	37	18.8
I-Tr 383	4.47	157.47	410	605	43	26.0
II-Tr 9c	0.28	25.62	425	383	84	6.7
I-Tr 291	0.16	8.78	430	326	99	2.7

liptinite macerals loosely and randomly dispersed within the mineral matrix. The overall liptinite contribution is 77%–99.7% (Fig. 5). Liptodetrinite (dimensions: 4 × 11 μm) is commonly observed. The lamalginite is quite short and straight with filaments or thread-like structures surrounding mineral particles (dimensions: 4 × 48 μm; Fig. 6H). Telalginite is very rare and occurs as singular objects (Fig. 6I). Vitrinite and inertinite (average contents 4.6% and 0.3%, respectively) are represented by angular vitrodetrinite and sharp-edged elongated

inertodetrinite (Fig. 6J).

The maceral assemblage in the sandstones' intercalation in the Dynów Marl Member is infrequent and highly scattered in the mineral matrix. The sandstones have high content of liptinite (in average 68.2%) and intermediate content of vitrinite (in average 29.4%). The liptinite macerals are mainly represented by angular liptodetrinite associated with lamalginite, which forms straight and wrapped filaments (average dimensions: 3 × 35 μm). The vitrodetrinite and inertodetrinite are usually angular and small-sized. Some inertinite macerals are elongated.

The green mudstone samples of the Krępak Member contain infrequent macerals that are chaotically scattered within mineral matrix. The maceral assemblage consists of vitrinite (in average 32.5%), inertinite (in average 21%) and liptinite (in average 46.5%) (Fig. 5). Most of vitrinite and inertinite are small and angular; however, singular larger pieces of telovitrinite with internal structure were also recognised (Fig. 6K). The liptinite macerals are mainly represented by liptodetrinite (dimensions: 3 × 15 μm). The lamalginite is filamentous (Fig. 6L), while telalginite is rare and ambiguous.

5. Discussion

5.1. Age determination

The age of the Dynów Marl Member in the section studied, based on nannofossils, is assigned to Zone NP23 due to the co-occurrence of abundant *Reticulofenestra ornata*, and very rare *Pontosphaera fibula* and *Reticulofenestra lockeri*. The assemblage is lacking *R. umbilica*, whose last occurrence marks the upper limit of Zone NP22. Such an association of species is characteristic of the equivalent of Zone NP23 in the Paratethys region (Nagymarosy and Voronina, 1992). The same age was proposed by Garecka (2012) from sediments overlying Chert Beds (= Dynów Marl Member) the Lower Menilite Beds.

The overlying green mudstones belong to Zone NP24. The zone assignment is based on the FO of *Cyclicargolithus abisectus*, which is usually found close to the FO of *S. ciperoensis* (zonal marker for the lower boundary of Zone NP24), and thus can be used to approximate the determination of the boundary of zones NP23 and NP24 (Martini and Műller, 1986). However, many authors believe that this species is already present in the lower part of NP23 (e.g., Bukry, 1973; de Kaenel and Villa, 1996; Maiorano and Monechi, 2006; Melinte-Dobrinescu and Brustur, 2008). The size of the coccoliths is significant; the smaller ones (less than 12 μm) are characteristic of NP23 and the lowest part of NP24 (see, for example, de Kaenel and Villa, 1996; Maiorano and Monechi, 2006; Śliwińska et al., 2012). In the samples from green mudstones, *Cyclicargolithus abisectus* is more than 12 μm in size. This indicates an age younger than the lowest part of Zone NP24. The other secondary index species are *S. dissimilis* and *H. carteri* (Fig. 4I– N), whose FO is characteristic for Zone NP24 (see Perch-Nielsen, 1985; Boesiger et al., 2017, respectively), and which were also observed in the assemblage.

However, such age determination is not in line with the stratigraphic scheme of the Menilite Formation in the Skole Nappe proposed by Kotlarczyk et al. (2006). According to Kotlarczyk et al. (2006)., the Dynów Marl Member was placed in the upper part of Zone NP22 and in the lowest part of Zone NP23, and correlated with the ichthyofaunal Zone IPM_1., whereas the green mudstones of the Krępak Member were positioned in the upper part of Zone NP23. No other unit was built of green mudstones in the Menilite Formation of the Skole Nappe. Therefore, the green mudstones from the Tarnawka section can be ascribed to the Krępak Member, with its new dating to Zone NP24. The same age (zone NP23) of the Dynów Marl Member of the Menilite Formation is known from the Fore-Magura, Ždánice-Subsilesian and Pouzdřany units of the Czech sector of the Outer Carpathians (Krhovský & Djurasinovič, 1993; Švábenická et al., 2007).

5.2. Depositional environment

The Paratethys Sea came into existence during the Early Oligocene. From the very beginning (calcareous nannoplankton Zone NP22), the water masses and their circulation were affected by both global and local climatic changes, occurring in an estuarine regime (Kováč et al., 2017b, and references therein). The thermohaline circulation was affected by fresh-water influx to the basin, resulting in the formation of strong halocline, and restricting vertical mixing. As a result, deficiency of oxygen at the bottom of the sea and the sedimentation of the euxinic facies occurred (cf. Tari et al., 1993; Krhovský, 1995; Leszczyński, 1997; Oszczypko-Clowes, 2001; Schulz et al., 2005; Soták, 2010).

According to Nagymarosy and Voronina (1992), *R. ornata* and *P. fibula* are characteristic of brackish-water environments and are limited to the Paratethys. The presence of abundant *R. ornata* and rare *P. fibula* is characteristic of the upper part of Zone NP23, and can be correlated with the Upper Solenovian Event from the Eastern Paratethys (the Greater Caucasus; see Nagymarosy and Voronina, 1992). This event is associated with the strong isolation and incursion of fresh waters in the Paratethys (Báldi, 1980; Rusu, 1988; Rögl, 1998). The present results show that the Solenovian Event also took place in the Skole Basin, as previously suggested by Studencka et al. (2016) on the basis of bivalves. The presence of *R. ornata* and *P. fibula* in the assemblages from the Dynów Marl Member of the Menilite Formation in the Tarnawka section reflects the freshwater run-off and inflow of fresh water carrying a large amount of organic matter. Organic material is so prominent here, as it was recorded in the Chert Member and the Dynów Marl Member of the Menilite Formation of the Ždánice-Pouzdřany Unit (Krhovský, 1981a, 1981b; Krhovský et al., 1992; Krhovský & Djurasinovič, 1993; Švábenická et al., 2007) and the Central Carpathian Paleogene Basin (Soták, 2010), as well as in the north-west Transylvania in bituminous marls and shales of the Bizuşa and Ileanda units, and in bituminous cherts, marls, and shales of the Menilite and the Lower Dysodile formations (Melinte, 2005; Melinte-Dobrinescu and Brustur, 2008).

Zone NP24 of the green mudstones from the Tarnawka section is characterised by the presence of rich and open-marine diversified assemblages dominated by *R. bisecta*, *Coccolithus pelagicus*, *Cyclicargolithus abisectus*, *Cyclicargolithus floridanus*, *H. compacta*, *H. carteri*, *H. ethologa* and *S. moriformis*. Typical low-salinity endemic Parathetyan species are rare. Such assemblages indicate that in Zone NP24, the normal salinity conditions in the Skole Basin were restored (see Garecka, 2012). At that time, the connection between the Paratethys and the North Sea, as well as with the Mediterranean region, was re-established (see Báldi, 1980; Rusu, 1988; Rögl, 1999).

Zone NP24 is characterised by the disappearance of the cold-water taxa, a growth in the abundance of warm-water taxa, and an increased number of reworked species. This could suggest the beginning of a warming episode in the younger Oligocene. This episode can be traced through the Carpathians in the Czech Republic (Krhovský, 1981a, 1981b; Krhovský et al., 1992; Krhovský & Djurasinovič, 1993; Švábenická et al., 2007), Poland (Oszczypko-Clowes, 2001; Oszczypko and Oszczypko-Clowes, 2009) and Romania (Melinte, 2005; Melinte--Dobrinescu and Brustur, 2008).

The amount and quality of organic matter differing in lithofacies agree with the interpretation of salinity changes inferred from the study of calcareous nannofossils. The maceral composition has been used to interpret salinity changes, through the assumption that long lamalginite and telalginite accompanied by amorphous organic matter refer to a saline environment (as in brown shales from the lower part of the Tarnawka section), whereas discrete liptinite represented by liptodetrinite and short lamalginite (present in marls of the Dynów Marl Member) is formed in waters with lower salinity (Liu et al., 2022). Highly carbonised vitrinite and inertinite predominate in green mudstones from the upper part of the section and sandstone intercalations. Vitrinite and inertinite are macerals of terrestrial origin derived from land-plant tissues and humic matter. Inertinites are oxidation products of other

macerals, e.g. carbonised plant tissues, oxidised resins (ICCP, 1998, 2001). Vitrinite and inertinite are fairly resistant to degradation. Thus, they are typical of a greater terrestrial influx. River transport is more favourable for the supply of vitrinite (Hackley et al., 2016; Shi-Ju et al., 2023), whereas the inertinite particles more readily experience aeolian transportation (Scott and Glasspool, 2007).

The brown shales from the lower part of the section consist of siliciclastics admixed with organic matter of aquatic and land-plant derivation. The Rock Eval data and the relationship between Tmax and HI (Espitalié et al., 1985) allow for the classification of the organic matter in the studied samples as oil-prone type II kerogen. The rocks are thermally immature. Similar Rock-Eval data have been previously obtained for the Menilite Formation, and the type II kerogen is considered to be primarily derived from algae and bacteria (e.g., Köster et al., 1998; Lewan et al., 2006; Kotarba et al., 2007; Waliczek and Więcław, 2012; Wendorff et al., 2017; Kosakowski et al., 2018).

Type II kerogen is dominated by liptinite macerals. The most frequent occurrence here is lamalginite, which shows a long, fibrous shape (Fig. 6A–C). Although dinoflagellate and acritarch cysts are considered to be the main source of most lamalginite in marine rocks, the lamellar-structured lamalginite from the investigated section could be of benthonic origin (cf. Pickel et al., 2017). Microbial mats in a saline environment may contribute to lamalginite, which occurs as long filaments (Hutton, 1987; Stasiuk, 1994). Such lamalginite is common in the studied brown shales, where it is accompanied by bituminite (Fig. 6A–C), which can be related to the bacterial transformation of organic matter in anoxic sediments. Telalginite occurs concomitantly in the studied brown shales and reveals the structure of colonial algae (Fig. 6B and C). Telalginite may have two algal sources: marine (e.g., *Tasmanites)* or fresh-water (*Botryococcus*) (Hutton, 1987). Typical *Tasmanites* have not been observed in the samples, although they have been described in the Menilite Shales (e.g., Ziemianin, 2018; Waliczek et al., 2022). The examined telalginite rather resembles *Botryococcus*, a freshwater algae that can also occur in sediments deposited in marine environments. The colonial algae of the chlorophyte genera, including *Botryococcus*, are common in the open Baltic Sea where the salinity ranges from 5 to 9‰ (Matthießen and Brenner, 1996). These algae are found in the sediments of the Black Sea and many other basins with salinity ranging from brackish to hypersaline (Mudie et al., 2010). The *Botryococcus* blooms after freshening of the saline basin by rain (Wake and Hillen, 1980), or by river-water inflow (e.g., Head, 1992). Therefore, telalginite, which may originated from marine algae and/or from the fresh-water *Botryococcus* has often been recognised in saline water deposits (Liu et al., 2022; Shi-Ju et al., 2023). The *Botryococcus* has been also described in the bituminous shales of the Menilite Formation and its analogue from the Romanian Outer Carpathians (Waliczek et al., 2022; Filipek, 2020).

The silty intercalations in the studied brown shales contain large pieces of vitrinite and inertinite with preserved cellular structure (Fig. 6E and F), which could be fluvially transported from land to the basin. Similar maceral features were recognised in many other Oligocene organic-rich shales in the Carpathians. Liptinite macerals associated with vitrinite (colotellinite and vitrodetrinite) and inetrinite (semifusinite and inertodetrinite) were recognised in the Menilite Shales (Waliczek and Więcław, 2012; Ziemianin, 2018, 2020; Waliczek et al., 2022). Their depositional conditions are interpreted as marine under the possible influence of riverine inflow (Wójcik-Tabol, 2015, 2017; Wójcik-Tabol et al., 2022). To conclude, the brown mudstones represent turbiditic and bottom current deposits enriched in planktonic and benthonic algal and bacterial organic matter produced massively in a marine environment, occasionally supplied in detritus by rivers.

The brackish water inflow during the deposition of the Dynów Marl Member is reflected in the maceral assemblages. Run-off-related low salinity might be indicated by the occurrence of terrestrial organic matter (Backman et al., 2006), represented here by vitrinite, inertinite and partly by liptodetrinite. Due to the prevailing hemipelagic sedimentation of the Dynów Marl Member, the vitrinite and inertinite are not abundant and small-sized. Ziemianin (2018) wrote that the content of vitrinite and inertinite in the micritic limestone of the Menilite Formation from the Skole Unit is low, and alginite is the most numerous. However, liptodetrinite dominates in the marl samples of the studied Dynów Marl Member. Liptodetrinite might consist of fragments of other liptinite macerals, including the terrestrial types (e.g., sporinite and cutinite), but liptodetrinite may also be interpreted as diatom resting spores and dinocysts (Stein et al., 2006). The appearance of diatom is usually linked to a high-productivity fertile environment likely related to an increase in the fluvial supply of nutrients. The diatoms in the Menilite Formation are broadly known (Kotlarczyk and Kaczmarska, 1987; Rospondek et al., 1997). The discrete lamalginite in the Dynów Marl Member (Fig. 6H) with simultaneously hardly noted telalginite (Fig. 6I) are an important salinity clue. The lamalginite contribution is thought to be associated with the desalination of surface waters (Liu et al., 2022; Shi-Ju et al., 2023). Discrete lamalginite could be derived from planktonic algae living in fresh-to-brackish water (Hutton, 1987). The macerals in the sandstone intercalations are infrequent and small, because they are dispersed in the mineral matrix. They are represented by highly fragmented detritus (probably redeposited) and subtle liptinite (lamalginite and liptodetrinite) originated from microplankton.

Few brown shales in the Dynów Marl Member are accompanied by sandstone layers. The HI values decrease here and indicate some variability of the organic matter. According to Wendorff et al. (2017), a reduction in hydrogen content is frequently observed in sedimentary sequences affected by deposition from turbiditic currents, which supply terrigenous organic matter to the central basin zone. However, it's worth noting that the decrease in HI can also result from oxidation during the transportation and redeposition of aquatic organic matter exposed to oxygenated water.

The Dynów Marl Member represents mostly a hemipelagic deposit influenced by gravity flows (represented by sandstone intercalations) and bottom currents (isolated siliciclastic laminae and thin layers). They consists mainly of calcium carbonate deriving primarily from nannoplankton and other microorganisms bloomed in brackish surface water. A stratified water column with high salinity and anoxic bottom waters are the major factors controlling depositional conditions. The carbonate content in the Dynów Marl Member decreases upward in section. A similar pattern of lowering content of calcite was described by Schulz et al. (2004) in the Dynów Marlstone (an equivalent of the Dynów Marl Member) of the Austrian Molasse Basin.

The green mudstones from the uppermost part of the section contain distinctly less macerals than the brown shales, and slightly more than in the Dynów Marl Member. Vitrinite (Fig. 6K) and inertinite predominate in them and indicate the influx from land. The association of organic matter is typical of a low-productivity and oxic environment. The sparse algal macerals represented by filamentous lamalginite (Fig. 6L) and the presumed presence of likely telalginite suggest the restoration of marine salinity.

6. Conclusions

1. On the basis of the calcareous nannoplankton, the age of the Dynów Marl Member is assigned to the Rupelian (Zone NP23), whereas the green mudstones (Krępak Member?) belong to Zone NP24.
2. Marls/marlstones/marly limestones of the Dynów Marl Member in the Skole Nappe are characterised by the presence of brackish water nannofossils, similarly to the NP23 deposits in the other parts of the Central and Eastern Paratethys. They record the maximum isolation of that bioprovince from the oceanic circulation (the Upper Solenovian Event).
3. Brown shales in the Boryslav Member were deposited by diluted turbidity and bottom currents supplying plant debris and fresh water algae. They are enriched in marine planktonic and benthonic algal and bacterial organic matter. The water body was probably

mesohaline–euhaline. Large aquatic macerals could also be related to good organic matter preservation in anoxic conditions.

4. The carbonate-dominated deposits of the Dynów Marl Member contain liptodetrinite and small lamalginite. They are mostly hemipelagic deposits settled down through a stratified water column with brackish surface waters and fully marine and anoxic bottom waters. The marls were deposited during the calcareous nannoplankton bloom. Consequently, the macerals are diluted by the carbonate groundmass.

Declaration of competing interest

The authors declare that they have no known competing financial interests or personal relationships that could have appeared to influence the work reported in this paper.

Data availability

Data will be made available on request.

Acknowledgements

This work has been supported by a grant from the Faculty of Geography and Geology under the Strategic Programme Excellence Initiative at Jagiellonian University. The authors wish to thank anonymous reviewers for their constructive criticism and detailed reviews of the manuscript. Special thanks go to Katarína Holcová for her most valuable comments, which have significantly improved the manuscript.

References

Backman, J., Moran, K., McInroy, D.B., Mayer, L.A., the Expedition 302 Scientists, 2006. Proceedings of the integrated ocean drilling program. Edinburgh 302, 115. https://doi.org/10.2204/iodp.proc.302.103.2006.

Báldi, T., 1980. The early history of Paratethys. Foldtani Kozlony 110, 456–472.

Bechtel, A., Hamor-Vido, M., Gratzer, R., Sachsenhofer, R.F., Püttmann, W., 2012. Facies evolution and stratigraphic correlation in the early Oligocene Tard Clay of Hungary as revealed by maceral, biomarker and stable isotope composition. Mar. Petrol. Geol. 35, 55–74. https://doi.org/10.1016/j.marpetgeo.2012.02.017.

Behar, F., Beaumont, V.D.E.B., Penteado, H.D.B., 2001. Rock-Eval 6 technology: performances and developments. Oil Gas Sci. Technol. 56, 111–134. https://doi.org/10.2516/ogst:2001013.

Belkin, H., Tewalt, S., Hower, J., Stucker, J.D., O'Keefe, J., Tatu, C., Buia, G., 2010. Petrography and geochemistry of Oligocene bituminous coal from the Jiu valley, Petroşani Basin (Southern Carpathian Mountains), Romania. Int. J. Coal Geol. 82, 68–80. https://doi.org/10.1016/j.coal.2010.01.013.

Boesiger, T.M., de Kaenel, E., Bergen, J.A., Browning, E., Blair, S.A., 2017. Oligocene to Pleistocene taxonomy and stratigraphy of the genus *Helicosphaera* and other placolith taxa in the circum North Atlantic Basin. J. Nannoplankt. Res. 37, 145–17.

Bojanowski, M.J., Ciurej, A., Haczewski, G., Jokubauskas, P., Schouten, S., Tyszka, J., Bijl, P.K., 2018. The Central Paratethys during Oligocene as an ancient counterpart of the present-day Black Sea: unique records from the coccolith limestones. Mar. Geol. 403, 301–328. https://doi.org/10.1016/j.margeo.2018.06.011.

Bojanowski, M.J., Oszczypko-Clowes, M., Barski, M., Oszczypko, N., Radzikowska, M., Ciesielska, Z., 2021. Slope destabilization provoked by dissociation of gas hydrates in the Outer Carpathian basin during the Oligocene: sedimentological, petrographic, isotopic and biostratigraphic record. Mar. Petrol. Geol. 123, 104585 https://doi.org/10.1016/j.marpetgeo.2020.104585.

Bośniacki, Z.G., 1911. Der europeische flysch. Kosmos 36, 871–899 ([In Polish, German summary]).

Bown, P.R., 1998. Calcareous Nannofossils Biostratigraphy. British Micropaleontological Society Publications Series, Chapman and Hall, Kluwer Academic Publishers, London, p. 314.

Bukry, D., 1973. Low-latitude coccolith biostratigraphic zonation. Initial Rep. Deep Sea Drill. Proj. 15, 127–149.

de Kaenel, E., Villa, G., 1996. Oligocene-Miocene calcareous nannofossil biostratigraphy and paleoecology from the Iberia Abyssal Plain. Proc. Ocean Drill. Progr. Sci. Results 149, 79–145. https://doi.org/10.2973/odp.proc.sr.149.208.1996.

Deuser, W.G., 1974. In: Degens, E.T., Ross, D.A. (Eds.), The Black Sea–Geology, Chemistry, and Biology, Memoir, 20. American Association of Petroleum Geologists, Tulsa, pp. 133–136.

Espitalié, J., Deroo, G., Marquis, F., 1985. La pyrolyse Rock-Eval et ses applications. Deuxième partie. Rev. Inst. Fr. Petrol 40, 755–784.

Filipek, A., 2020. Palynofacies analysis, sedimentology and hydrocarbon potential of the menilite beds (Oligocene) in the slovakian and Romanian outer Carpathians. Geol. Q. 64, 589–610. https://doi.org/10.7306/gq.1541.

Garecka, M., 2008. Oligocene/Miocene boundary in the Polish Outer Carpathians based on calcareous nannoplankton. Biul. Państwowego Inst. Geol. 432, 1–54 ([In Polish, with English summary).

Garecka, M., 2012. Record of the changes in the Oligocene-Miocene sediments of the Menilite-Krosno series of the Skole Unit based on calcareous nannoplankton studies-biostratigraphy and palaeogeographical implications (Polish Outer Carpathians). Biul. Państwowego Inst. Geol. 453, 1–22.

Golonka, J., Waśkowska, A., Ślączka, A., 2019. The western outer Carpathians: origin and evolution. Z. Dtsch. Ges. Geowiss. 170, 229–254. https://doi.org/10.1127/zdgg/2019/0193.

Hackley, P.C., Fishman, N., Wu, T., Baugher, G., 2016. Organic petrology and geochemistry of mudrocks from the lacustrine Lucaogou Formation, Santanghu Basin, northwest China: application to lake basin evolution. Int. J. Coal Geol. 168, 20–34. https://doi.org/10.1016/j.coal.2016.05.011.

Head, M.J., 1992. Zygospores of the zygnemataceae (division Chlorophyta) and other freshwater algal spores from the uppermost Pliocene St. Erth Beds of Cornwall, Southwestern England. Micropaleontology 38, 237–260. https://doi.org/10.2307/1485790.

Hutton, A.C., 1987. Petrographic classification of oil shales. Int. J. Coal Geol. 8, 203–231. https://doi.org/10.1016/0166-5162(87)90032-2.

ICCP, 1998. The new vitrinite classification (ICCP System, 1994). Fuel 77, 349–358. https://doi.org/10.1016/S0016-2361(98)80024-0.

ICCP, 2001. The new inertinite classification (ICCP System, 1994). Fuel 80, 459–471. https://doi.org/10.1016/S0016-2361(00)00102-2.

Jankowski, L., 2015. Nowe spojrzenie na budowę geologiczną Karpat – ujęcie dyskusyjne. Instytut Nafty i Gazu – Państwowy Instytut Badawczy, Kraków, p. 154 ([In Polish]).

Jankowski, L., Wysocka, A., 2019. Occurrence of clastic injectites in the Oligocene strata of the Carpathians and their significance in unravelling the Paleogene and Neogene evolution of the Carpathian orogeny (Poland, Ukraine and Romania). Geol. Q. 63, 106–125. https://doi.org/10.7306/gq.1460.

Jankowski, L., Kopciowski, R., Ryłko, W., Danysh, V., Tsarnenko, P.N., Hnylko, O., 2012. Lithostratigraphic correlation of the Outer Carpathian borderlands of Poland, Ukraine, Slovakia and Romania. Biul. Państwowego Inst. Geol. 449, 87–98.

Jarmołowicz-Szulc, K., Jankowski, L., 2011. Geochemical analysis and genetic correlation for bitumens and rocks of black shale type in the Outer Carpathians tectonic units in southeastern Poland and the adjacent territory. Biul. Państwowego Inst. Geol. 444, 73–98.

Jirman, P., Geršlová, E., Bubík, M., Sachsenhofer, R.F., Bechtel, A., Więcław, D., 2019. Depositional environment and hydrocarbon potential of the Oligocene Menilite Formation in the western Carpathians: a case study from the Loučka section (Czech Republic). Mar. Petrol. Geol. 107, 334–350. https://doi.org/10.1016/j.marpetgeo.2019.05.034.

Kosakowski, P., Koltun, Y., Machowski, G., Poprawa, P., Papiernik, B., 2018. The geochemical characteristics of the Oligocene–lower Miocene Menilite Formation in the Polish and Ukrainian outer Carpathians: a review. J. Petrol. Geol. 41, 319–335. https://doi.org/10.1111/jpg.12705.

Köster, J., Rospondek, M., Schouten, S., Kotarba, M., Zubrzycki, A., Damsté, J.S., 1998. Biomarker geochemistry of a Foreland Basin: the Oligocene Menilite Formation in the Flysch Carpathians of southeast Poland. Org. Geochem. 29, 649–669. https://doi.org/10.1016/S0146-6380(98)00182-X.

Kotarba, M.J., Więcław, D., Koltun, Y.V., Marynowski, L., Kuśmierek, J., Dudok, I.V., 2007. Organic geochemical study and genetic correlation of natural gas, oil and Menilite source rocks in the area between San and Stryi rivers (Polish and Ukrainian Carpathians). Org. Geochem. 38, 1431–1456. https://doi.org/10.1016/j.orggeochem.2007.03.012.

Kotlarczyk, J., 1988. Geologia Karpat przemyskich – "szkic do portretu". Przeglad Geol. 36, 325–333 ([In Polish]).

Kotlarczyk, J., Kaczmarska, I., 1987. Two diatoms horizons in the Oligocene and (?) lower Miocene of the Polish Outer Carpathians. Ann. Soc. Geol. Pol. 57, 143–188.

Kotlarczyk, J., Leśniak, T., 1990. Dolna część formacji menilitowej z poziomem diatomitów z Futomy w jednostce skolskiej polskich Karpat. Wydawnictwo Akademii Górniczo-Hutniczej, Kraków, p. 74 ([In Polish]).

Kotlarczyk, J., Uchman, A., 2012. Integrated ichnology and ichthyology of the Oligocene Menilite Formation, Skole and Subsilesian nappes, Polish Carpathians: a proxy to oxygenation history. Palaeogeogr. Palaeoclimatol. Palaeoecol. 331–332, 104–118. https://doi.org/10.1016/j.palaeo.2012.03.002.

Kotlarczyk, J., Jerzmańska, A., Świdnicka, E., Wiszniowska, T., 2006. A framework of ichthyofaunal ecostratigraphy of the Oligocene-Early Miocene strata of the Polish Outer Carpathian basin. Ann. Soc. Geol. Pol. 76, 111.

Kováč, M., Plašienka, D., Soták, J., Vojtko, R., Oszczypko, N., Less, Gy, Ćosović, V., Fügenschuh, B., Králiková, S., 2016. Paleogene palaeogeography and basin evolution of the Western Carpathians, Northern Pannonian domain and adjoining areas. Global Planet. Change 140, 9–27. https://doi.org/10.1016/j.gloplacha.2016.03.007.

Kováč, M., Hudáčková, N., Halásová, E., Kováčová, M., Holcová, K., Oszczypko-Clowes, M., Báldi, K., Less, G., Nagymarosy, A., Ruman, A., Klučiar, T., Jamrich, M., 2017a. The Central Paratethys palaeoceanography: a water circulation model based on microfossil proxies, climate, and changes of depositional environment. Acta Geologica Slovaca 9, 75–114.

Kováč, M., Márton, E., Oszczypko, N., Vojtko, R., Hók, J., Králiková, S., Plašienka, D., Klučiar, T., Hudáčková, N., Oszczypko-Clowes, M., 2017b. Neogene palaeogeography and basin evolution of the Western Carpathians, Northern Pannonian domain and adjoining areas. Global Planet. Change 155, 133–154. https://doi.org/10.1016/j.gloplacha.2017.07.004.

Krhovský, J., 1981a. Statigrafie a paleoekologie menilitového souvrství ždánické jednotky a diatomitů pouzdřanské jednotky. Zemny Plyn. a Nafta 26, 45–62 ([In Czech.]).

Krhovský, J., 1981b. Microbiostratigraphic correlations in the Outer Flysch Units of the southern Moravia and influence of the eustasy on their palaeogeographical development. Zemny Plyn. a Nafta 26, 665–688 and 955–975. [In Czech, with English summary].
Krhovský, J., 1995. Early Oligocene palaeoenvironmental changes in the West Carpathian Flysch Belt of Southern Moravia, vol. 4. Geological Society of Greece, Special Publication, pp. 209–213.
Krhovský, J., Djurasinović, M., 1993. The nannofossil chalk layers in the early Oligocene Stibořice member in Velké Němčice (the Menilitic Formation, Ždánice Unit, South Moravia): orbitally forced changes in paleoproductivity. Knih. Zemn. Plynu Naft. 15, 3–53.
Krhovský, J., Adamová, J., Hladíková, J., Maslowská, H., 1992. Paleoenviromental changes across the Eocene/Oligocene boundary in the Ždánice and Pouzdřany units (Western Carpathians, Czechoslovakia): the long- term trend and orbitally forced changes in calcarous nannofossil assemblages. In: Hamršmid, B., Young, J.R. (Eds.), Nannoplankton Research 2, Proceedings 4-th INA Conference, vol. 14b. Knihovnička ZPN, Prague, pp. 105–187.
Kruge, M.A., Mastalerz, M., Solecki, A., Stankiewicz, B.A., 1996. Organic geochemistry and petrology of oil source rocks, Carpathian Overthrust region, southeastern Poland—implications for petroleum generation. Org. Geochem. 24, 897–912. https://doi.org/10.1016/S0146-6380(96)00067-8.
Książkiewicz, M., 1977. The tectonics of the Carpathians. In: Pożaryski, W. (Ed.), Geology of Poland, 4. Tectonics. Wydawnictwa Geologiczne, Warszawa, pp. 476–699.
Leszczyński, S., 1997. Origin of the sub- menilite Globigerina marl (Eocene-Oligocene transition) in the Polish Outer Carpathians. Ann. Soc. Geol. Pol. 67, 367–427.
Lewan, M.D., Kotarba, M.J., Curtis, J.B., Więcław, D., Kosakowski, P., 2006. Oil-generation kinetics for organic facies with type-II and -IIs kerogen in the Menilite Shales of the Polish Carpathians. Geochimica et Cosmochimica 70, 3351–3368. https://doi.org/10.1016/j.gca.2006.04.024.
Lityński, T., Jurkowska, H., Gorlach, E., 1976. Chemical and Agriculture Analysis. PWN, Warszawa, p. 129 ([In Polish]).
Liu, S., Gao, G., Jin, J., Gang, W., Xiang, B., 2022. Source rock with high abundance of C28 regular sterane in typical brackish-saline lacustrine sediments: biogenic source, depositional environment and hydrocarbon generation potential in Junggar Basin, China. J. Petrol. Sci. Eng. 208, 109670 https://doi.org/10.1016/j.petrol.2021.109670.
Maiorano, P., Monechi, S., 2006. Early to late Oligocene calcareous nannofossil bioevents in the Mediterranean (Umbria-Marche basin, central Italy). Riv. Ital. Paleontol. Stratigr. 12, 261–273. https://doi.org/10.13130/2039-4942/6340.
Malata, T., 1996. Analiza formalnych wydzieleń litostratygraficznych oraz propozycja podziału jednostki skolskiej polskich Karpat fliszowych. Przegląd Geol. 44, 509–514 ([In Polish]).
Malata, T., 2006. Warstwy menilitowe w kamieniołomie w Tarnawce. Kraków. In: Słomka, T., Doktor, M., Joniec, A., Kicińska-Świderska, A. (Eds.), Katalog Obiektów Geoturystycznych W Polsce. Wydawnictwa Akademii Górniczo-Hutniczej, pp. 158–159 ([In Polish]).
Martini, E., 1971. Standard Neogene calcareous nannoplankton zonation. Nature 225, 289–290. https://doi.org/10.1038/225289a0.
Martini, E., Műller, C., 1986. Standard Tertiary and Quaternary calcareous nannoplankton zonation. In: Farinacci, A. (Ed.), Proceedings of the Second Planktonic Conference Roma 1970, pp. 737–785. https://doi.org/10.1127/nos/16/1986/99. Rome.
Matthießen, J., Brenner, W., 1996. Chlorococcalalgen und Dinoflagellaten-Zysten in rezenten Sedimenten des Greifswalder Boddens (südliche Ostsee). Senckenberg. Maritima 27, 33–34 8.
Melinte, M.C., 2005. Oligocene palaeoenvironmental changes in the Romanian Carpathians, revealed by calcareous nannofossils. Stud. Geol. Pol. 124, 341–352.
Melinte-Dobrinescu, M., Brustur, T., 2008. Oligocene - lower Miocene events in Romania. Acta Palaeontologica Romaniae 6, 203–215.
Miclăus, C., Loiacono, F., Puglisi, D., Baciu, D., 2009. Eocene-Oligocene sedimentation in the external areas of the Moldavide Basin (Marginal Folds Nappe, Eastern Carpathians, Romania): sedimentological, paleontological and petrographic approaches. Geol. Carpathica 60, 397–417.
Mudie, P.J., Marret, F., Rochon, A., Aksu, A.E., 2010. Non-pollen palynomorphs in the Black Sea corridor. Veg. Hist. Archaeobotany 19, 531–544. https://doi.org/10.1007/s00334-010-0268-9.
Nagymarosy, A., Voronina, A., 1992. Calcareous nannoplankton from the lower Maykopian beds (early Oligocene, union of independent states). In: Hamrsmid, B., Young, J. (Eds.), Nannoplankton Research 2, Proceedings 4-th INA Conference, vol. 14b. Knihovnička Zemni Plyn a Nafta, Prague, pp. 187–221, 1991.
Nalivkin, D.W., 1963. Flysch – continental deposit. Asociatia Geologica Carpato-Balcanica, Congresul, Bucuresti 3, 67–73 ([In Russian]).
Nalivkin, D.W., 1967. Fauna in the flysch area of the Polish Carpathian Mts. Kwart. Geol. 11, 866–876.
Oszczypko, N., 1999. From remnant oceanic basin to collision-related foreland basin-a tentative history of the Outer Western Carpathians. Geol. Carpathica 50 (special issue), 161–163.
Oszczypko, N., 2006. Late Jurassic–Miocene evolution of the Outer Carpathian fold-and-thrust belt and its foredeep basin (western Carpathians, Poland). Geol. Q. 50, 169–193.
Oszczypko, N., Oszczypko-Clowes, M., 2009. Stages in the Magura Basin: a case study of the Polish sector (Western Carpathians). Geodin. Acta 22, 83–100. https://doi.org/10.3166/ga.22.83-100.
Oszczypko-Clowes, M., 2001. The nannofossil biostratigraphy of the youngest deposits of the Magura Nappe (east of the Skawa river, Polish Flysch Carpathians) and their palaeoenviromental conditions. Ann. Soc. Geol. Pol. 71, 139–188.
O'Brien, C.L., Huber, M., Thomas, E., Pagani, M., Super, J.R., Elder, L.E., Hull, P.M., 2020. The enigma of Oligocene climate and global surface temperature evolution. Proc. Natl. Acad. Sci. USA 117, 25302–25309. https://doi.org/10.1073/pnas.2003914117.
Perch-Nielsen, K., 1985. Cenozoic calcareous nannofossils. In: Bolli, H., Saunders, J.S., Perch-Nielsen, K. (Eds.), Plankton Stratigraphy, vol. 11. Cambridge University Press, pp. 427–554.
Pickel, W., Kus, J., Flores, D., Kalaitzidis, S., Christanis, K., Cardott, B.J., Misz-Kennan, M., Rodrigues, S., Hentschel, A., Hamor-Vidoh, M., Crosdale, P., Wagner, N., ICCP., 2017. Classification of liptinite–ICCP system 1994. Int. J. Coal Geol. 169, 40–61. https://doi.org/10.1016/j.coal.2016.11.004.
Lithological paleogeographic maps of paratethys-10 maps late Eocene to pliocene. In: Popov, S.V., Rögl, F., Raznov, A.Y., Steininger, F.F., Shcherba, I.G., Kovac, M. (Eds.), Cour. Forschungsinst. Senckenberg 250, 1–42.
Puglisi, D., Badescu, D., Carbone, S., Corso, S., Franchi, R., Gigliuto, L., Loiacono, F., Miclăus, C., Moretti, E., 2006. Stratigraphy, petrography and palaeogeographic significance of the early Oligocene "menilite facies" of the Tarcau Nappe (Eastern Carpathians, Romania). Acta Geol. Pol. 56, 105–120.
Rajchel, J., 1990. Lithostratigraphy of the Upper Palaeocene and Eocene sediments from the Skole unit. Zeszyty Naukowe Akademii Górniczo-Hutniczej- Geologia 48, 1–112 ([In Polish, with English summary]).
Rauball, J.F., Sachsenhofer, R.F., Bechtel, A., Coric, S., Gratzer, R., 2019. The Oligocene–Miocene Menilite Formation in the Ukrainian Carpathians: a world-class source rock. J. Petrol. Geol. 42, 393–416. https://doi.org/10.1111/jpg.12743.
Rögl, F., 1998. Palaeogeographic considerations for Mediterranean and Paratethys seaways (Oligocene to Miocene). Ann. Nathist Mus Wien 99A, 279–310. https://doi.org/10.2307/41702129.
Rögl, F., 1999. Mediterranean and Paratethys. Facts and hypotheses of an Oligocene to Miocene paleogeography (short overview). Geol. Carpathica 50, 339–349.
Roth, P.H., Thierstein, H., 1972. Calcareous nannoplankton: Leg 14 of the Deep Sea Drilling Project. In: Hayes, D.E., Pimm, A.C., et al. (Eds.), Initial Reports Deep Sea Drilling Project, 14.
Rospondek, M.J., Köster, J., Damsté, J.S., 1997. Novel C26 highly branched isoprenoid thiophenes and alkane from the Menilite Formation, Outer Carpathians, SE Poland. Org. Geochem. 26, 295–304. https://doi.org/10.1016/S0146-6380(97)00021-1.
Rusu, A., 1988. Oligocene events in Transylvania (Romania) and the first separation of Paratethys. Dari de Seama ale Institutului de Geologie şi Geofizică 72–73, 207–223.
Sachsenhofer, R.F., Stummer, B., Georgiev, G., Dellmour, R., Bechtel, A., Gratzer, R., Ćorić, S., 2009. Depositional environment and hydrocarbon source potential of the Oligocene Ruslar Formation (kamchia depression; western Black Sea). Mar. Petrol. Geol. 26, 57–84. https://doi.org/10.1016/j.marpetgeo.2007.08.004.
Sachsenhofer, R.F., Bechtel, A., Gratzer, R., Rainer, T.M., 2015. Source-rock maturity, hydrocarbon potential and oil–source-rock correlation in well shorish-1, Erbil province, Kurdistan region, Iraq. J. Petrol. Geol. 38, 357–381. https://doi.org/10.1111/jpg.12617.
Salata, D., Uchman, A., 2012. Heavy minerals from Oligocene sandstones of the Menilite Formation of the Skole Nappe, SE Poland: a tool for provenance specification. Geol. Q. 56, 803–812. https://doi.org/10.7306/gq.1056.
Salata, D., Uchman, A., 2019. New interpretation of the provenance of crystalline material from Oligocene flysch deposits of the Skole Nappe, Poland: evidence from heavy minerals and clasts in the Nowy Borek section. Geologos 25, 163–174. https://doi.org/10.2478/logos-2019-0015.
Schmid, S.M., Bernoulli, D., Fügenschuh, B., Matenco, L., Schefer, S., Schuster, R., Tischler, M., Ustaszewski, K., 2008. The Alpine-Carpathian-Dinaridic orogenic system: correlation and evolution of tectonic units. Swiss J. Geosci. 101, 139–183. https://doi.org/10.1007/s00015-008-1247-3.
Schulz, H.M., Bechtel, A., Rainer, T., Sachsenhofer, R.F., Struck, U., 2004. Paleoceanography of the western central Paratethys during early Oligocene nannoplankton zone NP23 in the Austrian Molasse Basin. Geol. Carpathica 55, 311–323.
Schulz, H.M., Bechtel, A., Sachsenhofer, R.F., 2005. The birth of the Paratethys during the early Oligocene: from Tethys to an ancient Black Sea analogue? Global Planet. Change 49, 163–176. https://doi.org/10.1016/j.gloplacha.2005.07.001.
Scott, A.C., Glasspool, I.J., 2007. Observations and experiments on the origin and formation of inertinite group macerals. Int. J. Coal Geol. 70, 53–66. https://doi.org/10.1016/j.coal.2006.02.009.
Shi-Ju, L., Gao, G., Wenzhe, G., Baoli, X., Ming, W., 2023. Differences in geochemistry and hydrocarbon generation of source-rock samples dominated by telalginite and lamalginite: a case study on the Permian saline lacustrine source rocks in the Jimusaer Sag, NW China. Petrol. Sci. 20, 141–160. https://doi.org/10.1016/j.petsci.2022.08.034.
Śliwińska, K.K., Abrahamsen, N., Beyer, C., Brünings-Hansen, T., Thomsen, E., Ulleberg, K., Heilmann-Clausen, C., 2012. Bio- and magnetostratigraphy of Rupelian–mid Chattian deposits from the Danish land area. Rev. Palaeobot. Palynol. 172, 48–69. https://doi.org/10.1016/j.revpalbo.2012.01.008.
Soták, J., 2010. Paleoenvironmental changes across the Eocene-Oligocene boundary: insight from the Central-Carpathian Paleogene Basin. Geol. Carpathica 61, 393–418. https://doi.org/10.2478/v10096-010-0024-1.
Stasiuk, L.D., 1994. Oil-prone alginite macerals from organic-rich Mesozoic and Palaeozoic strata, Saskatchewan, Canada. Mar. Petrol. Geol. 11, 208–217. https://doi.org/10.1016/0264-8172(94)90097-3.
Stein, R., Boucsein, B., Meyer, H., 2006. Anoxia and high primary production in the Paleogene central Arctic Ocean: first detailed records from Lomonosov Ridge. Geophys. Res. Lett. 33, L18606 https://doi.org/10.1029/2006GL026776.
Strakhov, N.M., 1971. Geochemical evolution of the Black Sea in the Holocene. Litologia i Poleznye Iskopayemy,e 3, 3–17 ([In Russian, English title]).

Strakhov, N.M., 1976. Problems of the geochemistry of recent oceanic lithogenesis. Tr. - Geol. Inst. Akad. Nauk. SSSR 292, 1–299 ([In Russian, English title]).

Studencka, B., Popov, S.V., Bieńkowska-Wasiluk, M., Wasiluk, R., 2016. Oligocene bivalve faunas from the Silesian Nappe, Polish Outer Carpathians: evidence for the early history of the Paratethys. Geol. Q. 60, 317–340. https://doi.org/10.7306/gq.1296.

Švábenická, L., Bubík, M., Stráník, Z., 2007. Biostratigraphy and paleoenvironmental changes on the transition from the Menilite to Krosno lithofacies (Western Carpathians, Czech Republic). Geol. Carpathica 58, 237–262.

Tari, G., Báldi, T., Báldi-Beke, M., 1993. Paleogene retroarc flexural basin beneath the Neogene Pannonian Basin: a geodynamic model. Tectonophysics 226, 433–455. https://doi.org/10.1016/0040-1951(93)90131-3.

Unrug, R., 1980. Ancient contourites in the menilite beds (Oligocene) of the Carpathian flysch, Poland. Rocz. Pol. Tow. Geol. 50, 175–182.

Vető, I., 1987. An Oligocene sink for organic carbon: upwelling in the Parathetys? Palaeogeogr. Palaeoclimatol. Palaeoecol. 60, 143–153.

Wake, L.V., Hillen, L.W., 1980. Study of a "bloom" of the oil-rich alga *Botryococcus braunii* in the Darwin River Reservoir. Biotechnol. Bioeng. 22, 1637–1656. https://doi.org/10.1002/bit.260220808.

Waliczek, M., Więcław, D., 2012. Maturity of Menilite shales from Polish Outer Carpathians based on vitrinite reflectance and rock-eval pyrolysis data. Geology, Geophysics and Environment 38, 551–552.

Waliczek, M., Machowski, G., Solecki, M.L., Stefaniuk, M., 2022. An evaluation of organic matter dispersed in the Menilite Formation in Silesian Nappe (Polish Outer Carpathians): an optical microscopic approach. Geology, Geophysics and Environment 48, 243–256. https://doi.org/10.7494/geol.2022.48.3.243.

Wdowiarz, S., 1949. Structure géologique des Karpates Marginales au sudest de Rzeszów. Biuletyn Państwowego Instytutu Geologicznego, 11, pp. 1–51 [In Polish, French summary].

Wendorff, M., Rospondek, M.J., Kluska, B., Marynowski, L., 2017. Organic matter maturity and hydrocarbon potential of the lower Oligocene menilite facies in the Eastern Flysch Carpathians (Tarcău and Vrancea nappes), Romania. Appl. Geochem. 78, 295–310. https://doi.org/10.1016/j.apgeochem.2017.01.009.

Wójcik-Tabol, P., 2015. Depositional redox conditions of the Grybów Succession (Oligocene, Polish Carpathians) in the light of petrological and geochemical indices. Geol. Q. 59, 603–614. https://doi.org/10.7306/gq.1240.

Wójcik-Tabol, P., 2017. Elemental and organic carbon proxies for redox conditions of the Oligocene formations in the Ropa Tectonic Window (Outer Carpathians, Poland): palaeoenvironmental implications. Ann. Soc. Geol. Pol. 87, 41–53. https://doi.org/10.14241/asgp.2017.005.

Wójcik-Tabol, P., Wendorff-Belon, M., Kosakowski, P., Zakrzewski, A., Marynowski, L., 2022. Paleoenvironment, organic matter maturity and the hydrocarbon potential of Menilite shales (Silesian Unit, Polish Outer Carpathians)–Organic and inorganic geochemical proxies. Mar. Petrol. Geol. 142, 105767 https://doi.org/10.1016/j.marpetgeo.2022.105767.

Zachos, J.C., Pagani, M., Sloan, L., Thomas, E., Billups, K., 2001. Trends, rhythms, and aberrations in global climate 65 Ma to present. Science 292, 686–693.

Zielińska, M., Fabiańska, M., Więcław, D., Misz-Kennan, M., 2020. Comparative petrography and organic geochemistry of different types of organic matter occurring in the Outer Carpathians rocks. Geol. Q. 64, 165–184. https://doi.org/10.7306/gq.1523.

Ziemianin, K., 2018. Characteristics of dispersed organic matter in the Menilite beds from the Skole Unit. Nafta Gaz. 74, 636–646. https://doi.org/10.18668/NG.2018.09.02.

Ziemianin, K., 2020. Characteristics of dispersed organic matter in selected lithostratigraphic divisions within the Skole Unit (Carpathian Mts., SE Poland). Nafta Gaz. 76, 669–678.

Żytko, K., Zając, R., Gucik, S., Ryłko, W., Oszczypko, N., Garlicka, I., Nemčok, J., Eliáš, M., Menčik, E., Stránik, Z., 1989. Map of the tectonic elements of the Western Outer Carpathians and their foreland 1:500 000. In: Poprawa, D., Nemčok, J. (Eds.), Geological Atlas of the Western Outer Carpathians and their Foreland. Państwowy Instytut Geologiczny Warszawa/GUDŠ Bratislava/Uug Praha.